NEUTRON SHIELDING PROPERTIES OF MORTARS CONTAINING HAYDITE AGGREGATE

by

Marvin Leonard Duke

A Thesis Submitted to the
Graduate Faculty in Partial Fulfillment of
The Requirements for the Degree of
MASTER OF SCIENCE

Major Subject: Nuclear Engineering

Signatures have been redacted for privacy

Iowa State College
Ames, Iowa
1959

TABLE OF CONTENTS

I. INTRODUCTION

A. Use of Concrete as a Shield

The process involving shielding had not been completely understood for many years after the completion of the first reactor. Most energy and study had been applied to the reactor core, and the simple empirical methods of shield design could be utilized to give a workable and safe shield, even though it might be excessively heavy and expensive. At the present time, with the realization that nuclear power will have to compete with and eventually replace conventional power methods, the problem of low cost and low weight shielding has become quite important.

A natural choice for shielding material exhibiting both qualities of low cost and low weight is concrete, and, consequently, it has become the most widely used material for reactor shielding. Its popularity has also been enhanced by its satisfactory mechanical properties as well as its ideal radiation shielding attributes. It contains hydrogen and other light nuclei as well as nuclei of fairly high atomic number. The light elements moderate the neutrons, and the heavier elements absorb the gamma radiation. Recent developments have brought about the utilization of heavy concretes containing barytes and iron ore for additional gamma ray attenuation.

B. Neutron Attenuation

The attenuation of fast neutrons in a shield can be attributed to three successive processes:

1. Collision, either inelastic or elastic, and involving significant change of direction or energy degradation or both (elastic forward scattering attenuates very little).
2. Slowing down by many collisions, mostly elastic.
3. Diffusion at or near thermal energy to absorption.

A collision with hydrogen usually has nearly the effect of absorption. Qualitatively this is true because of the degradation in energy which accompanies the collision, combined with the rapid increase of the hydrogen cross section as the neutron energy decreases, which is shown on Figure 1. A small fraction of the initial collisions with hydrogen will give rise to neutrons having very nearly the source energy and almost their original direction. These neutrons will penetrate nearly as well as uncollided neutrons.

A neutron may also collide with a heavy nucleus. There may result an approximately isotropic emission of neutrons with an energy spectrum which depends on the energy of the incident neutron. For energies below 1 mev, the scattering will usually be elastic, while, as the energy rises, the scattering becomes predominantly inelastic.

At low energies, with isotropic elastic scattering predominating, a neutron collision changes the direction of the

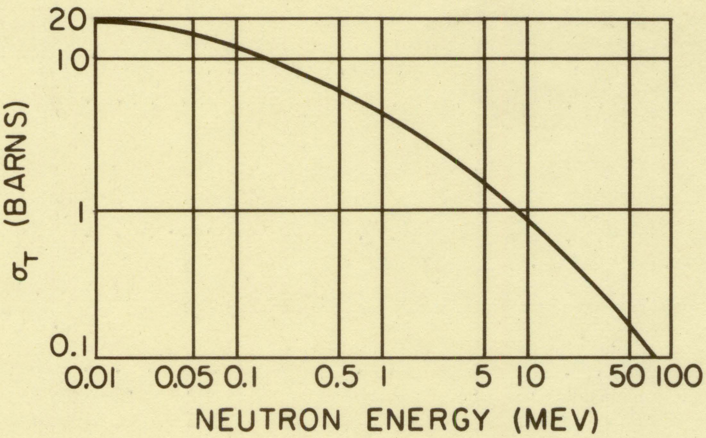

Figure 1. Total cross-section of hydrogen
Price (12, p. 117)

neutron effectively so that it gives a small contribution at the outside of a thick shield.

At higher energies, about one-half the total cross section of the heavy elements corresponds to small angle elastic deflections.

These deflections are associated with the diffracted neutron shadow cast by the opaque nucleus. At low energies, 1 to 2 Mev, this cross section may be treated as isotropic and therefore included as an absorption. At higher energies, the total shadow scattering is included in a small angular range and is ineffective in removing neutrons.

In a thermal reactor, slow neutrons are much more numerous than the fast components (Energy greater than .5 Mev), are more rapidly attenuated, and their effect is felt only in that portion of the shield in proximity to the source. They have, therefore, little to do with the calculations on required shield thickness, though they do play an important part in computing heat effects on the inner part of the reactor shield.

The processes by which fast neutrons are attenuated in thick shields are quite complex. The exact calculations of the variation of fast neutron flux with shield thickness and the determination of the flux of neutrons of lower energy resulting from fast neutron collisions are difficult mathematically.

A semi-empirical method which, under the proper conditions, gives excellent results in predicting neutron attenuation was evolved by Albert and Welton (1). Their removal cross section theory takes into account the removal of fast neutrons due to reactions, capture, inelastic scattering, and elastic scattering not in the shadow. The conditions under which this cross section may be used are the following; first, the neutron source must have a fission spectrum, as shown on Figure 2, which has an average energy of about 2 Mev. Secondly, the material must be followed by a large thickness of hydrogenous material or must be intimately mixed with such material. Glasstone (6, p. 617) states that the weight of a shield must be at least 10 per cent water in order to provide the minimum proportion of hydrogen for application of the theory. It has been shown that the fission spectrum falls off rapidly at high energies, while hydrogen is an increasingly efficient attenuator of neutrons as the energy is decreased. These two phenomena work to restrict to a narrow energy band those source neutrons responsible for the dose at large distances in a hydrogenous medium. The band lies in an energy region usually 6 to 10 Mev, depending on the material, where neutron collisions with many substances either have no significant effect on the neutron or act as absorptions. In these circumstances, the substances act as simple absorbers with apparent absorption or removal cross sections

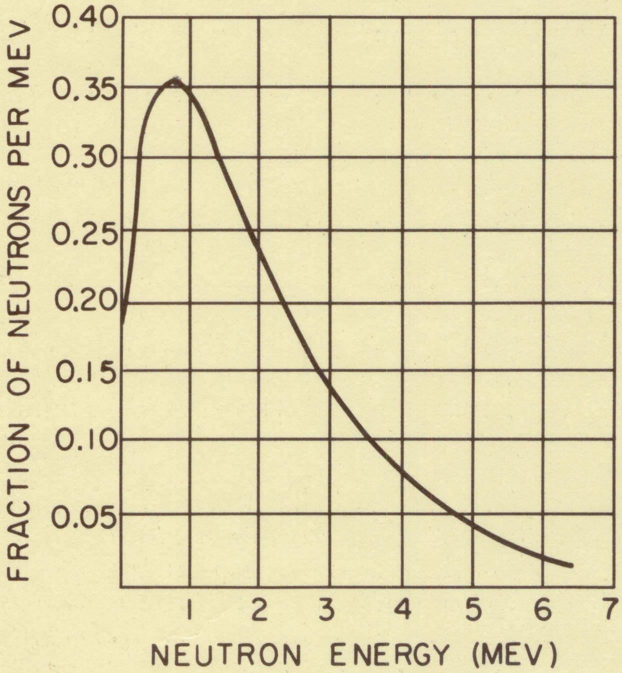

Figure 2. Fission neutron energy distribution
Murray (11, p. 57)

which are independent of the thickness of the media.

The removal cross section is determined by putting a slab of the material, for which the cross section is to be found, of x cm thickness in a tank consisting of z cm of water. If Do(z) is the dose rate observed from a given source through the water only, then the dose rate D(z,x) from the same source for the shield consisting of water and slab will be

$$D(z,x) = e^{-\Sigma_r x} Do(z)$$

where Σ_r cm^{-1} is the effective macroscopic removal cross section of the material which is related to the effective microscopic removal cross section, σ_r, in the usual manner.

The fast neutron removal attenuation length, λ_r, the reciprocal of the macroscopic fast neutron removal cross section, is the distance for an e-fold reduction in the fast neutron flux.

II. REVIEW OF LITERATURE

Rockwell (13) discusses the properties of various concrete shielding blocks and brick composed of different heavy aggregates. He states that the main purpose of cements is to provide hydrogen, bonding strength, and, if possible, a reasonably high density.

Gallaher and Kitzes (5) reported on the experimental programs which were conducted at the Oak Ridge National Laboratory on Portland cement concretes tested for suitability for reactor shielding. They listed the following desired properties necessary for effective shields:

1) High density to minimize thickness

2) High hydrogen content to thermalize intermediate neutrons

3) High content of heavy elements for degradation of fast neutrons as well as gamma rays

4) Low cost of ingredients

5) Ease of mixing and placing the concrete.

In addition, structural strength, stability under radiation and stability under hot moist or dry conditions were also considered. The article also discusses the handling and pouring techniques to be used with heavy aggregate concrete as well as concretes with high water content.

Price and Horton (12, p. 284) state that the total cross section per unit weight for fast neutrons is considerably greater for light elements than for heavy elements; and it follows that the most efficient fast neutron shields (on a weight basis) are those containing large amounts of hydrogen. The most obvious choice then, for an effective fast neutron attenuator, is water, and, even though many materials contain more hydrogen per unit volume, their use is governed by considerations such as flammability, liability to radiation damage, and chemical and thermal stability.

An experiment to determine the effect of water in structural concrete on the attenuation of intermediate energy neutrons (epithermal to 1 Mev) was conducted by Blizzard and Miller (3). It was found that a 7 per cent water content is adequate to insure that intermediate energy neutrons be quickly slowed down to thermal energy where they are readily captured. The attenuation of the neutrons in the water moderated concrete shield was found to follow an exponential function with the fast neutron macroscopic removal cross section for the attenuation coefficient. A greater water content improved the over-all neutron attenuation according to the removal cross section theory.

One of the oldest existing shields is the concrete shield around the Oak Ridge National Laboratory Graphite Reactor. This shield consists of a five foot thickness of bituminous painted concrete consisting of 16.3% Portland cement, 27.3% haydite, 46.4% barytes, and 10% water, sandwiched between two 1-foot thicknesses of ordinary Portland concrete. An investigation of the physical properties of the shield was performed between February and July 1956, after the shield had been in place 12 years, and the results were reported by Blosser and associates (4). The investigation showed that the chemical properties and density of the shield had not changed appreciably since a similar investigation made in 1948 when the water content was still nearly five times normal and no radiation damage was detectable. The compressive strength was lower, however, reaching a maximum change of about 40% near the reflector shield interface.

A report issued by the Housing and Home Finance agency (14) indicates that haydite is one of the best of the lightweight aggregates, and that haydite concrete may be used in place of typical Portland cement concrete without discounting the design in any degree for strength, workability, and durability. Furthermore, it provides a saving in dead weight of about 30%.

III. INVESTIGATION

The use of haydite (a light porous, calcined shale capable of absorbing large quantities of water) as an aggregate was studied to determine the effect of the haydite and absorbed water on the fast and thermal neutron attenuation properties of mortars and concretes.

Water is a good neutron moderator, and it has been shown that the large amount of water absorbed by the haydite may be retained over a long period of time if the concrete is properly coated.

As was shown previously, in water there is a strong variation in total cross section with neutron energy; however, the total cross section for Portland concrete does not vary so markedly for low and high energies, see Figure 3.

The study of the neutron shielding effectiveness of haydite mortar and concrete consisted of two main parts. The first was the determination of the effect of changing the amount of haydite in the concrete and mortar on the shielding effectiveness. The second part was the determination of the neutron shielding effectiveness of a concrete containing a large percentage of haydite as a function of the amount of water absorbed.

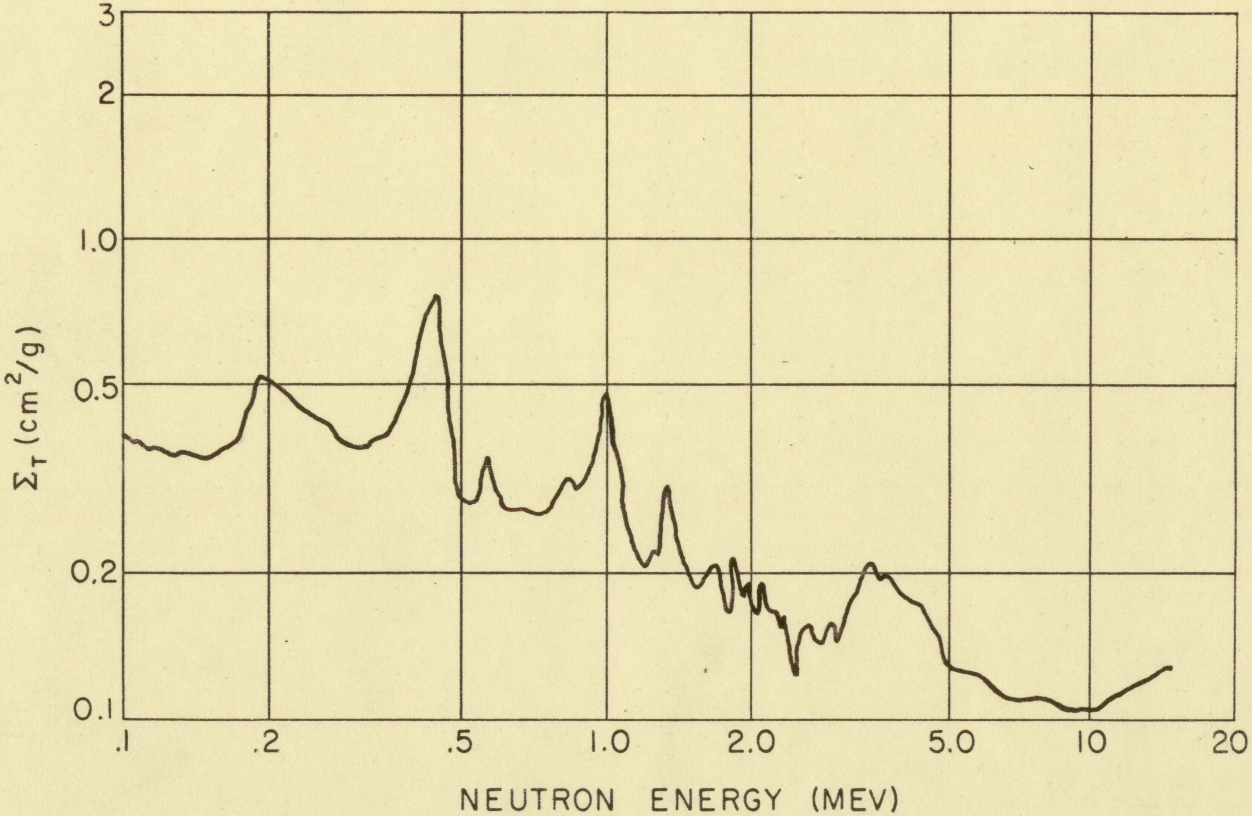

Figure 3. Total macroscopic neutron cross sections for Portland cement concrete
Blizzard and Miller (3, p. 20)

IV. EQUIPMENT AND MATERIAL

A. Radiation Source

A plutonium-beryllium source containing 16 gm. of plutonium of approximately 1-curie strength provided the neutrons used in this study. The plutonium and beryllium were mixed together and sealed in a tantalum and stainless steel right circular cylinder of 1.35 in. height and 1.02 in. diameter. The average number of neutrons given off by this source is 1.65×10^6 each second, and the energy distribution of the neutrons is shown on Figure 4.

The source was placed on top of a wooden block which was inside a tight fitting teflon cylindrical container. The teflon cylinder fit tightly within the steel pipe housing of the original shipping container which was encased in paraffin on all sides but the top two inches. In this manner a vertical collimated source of neutrons was obtained, see Figure 5.

B. Shielding Materials

The shielding materials used were 2 by 2 by 4 inch mortar blocks. The composition of the blocks was varied by changing the weight of aggregate and sand in each mixture and keeping the total weight of all the components constant. The fabrication and composition of the blocks is discussed in the

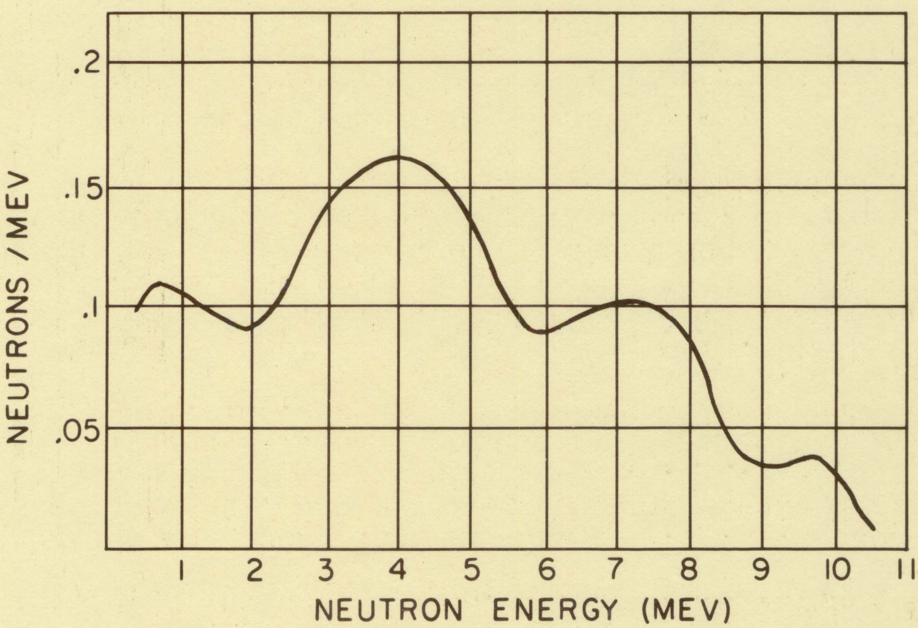

Figure 4. Energy distribution of neutrons emitted from a plutonium-beryllium source (the area under the curve has been normalized to unity)
Price (12, p. 151)

Figure 5. Source housing and detector

A. Teflon cylinder
B. Paraffin surrounded steel pipe
C. BF_3 neutron counting tube
E. Steel shipping container shrouded by cadmium


E
A
B
C

section on procedures. A chemical analysis of the components was not obtained. However, Table 1 indicates the normal composition of Portland cement and the assumed composition of the haydite aggregate used in the Oak Ridge graphite reactor shield.

Table 2 shows the aggregate and sand particle distribution as determined by sieve analysis.

Table 1. Chemical composition of cement and aggregate in per cent weight

	SiO_2	Fe_2O_3	Al_2O_3	CaO	MgO	
Portland cement type I[a]	23	4	8	63	2	
	SiO_2	Al_2O_3	CaO	Al	Ca	Si
Haydite aggregate[b]	60	16	24	8.5	17.0	48

[a]Average values from Hungerford (9, p. 723).

[b]Blosser and associates (4, p. 7).

C. Detector and Apparatus

The detector used was a standard N. C. Wood BF_3 neutron proportional counter, catalog number G1174. The active counting volume was 1 in. in diameter and 6 in. in length. The BF_3 gas was enriched to 96% Boron 10 and was under a pressure of 40 cm. Hg. A $B^{10}F_3$ counter has a very high neutron detection efficiency. The total cross section, σ_t, is 3960

Table 2. Grading of aggregate and sand. Sieve analyses, per cent by weight passing U. S. standard sieves

	No. 4	No. 8	No. 14	No. 28	No. 50	No. 100
Sand	99	94	75	76	9	0
			1/2 in.	3/8 in.	No. 4	No. 8
Haydite aggregate			100	98	12	0

barns at neutron energies of .025 ev. The ions which are counted come from the alpha particles produced by the following reaction:

$$B^{10} + n \rightarrow Li^{7} + \alpha$$

The proportional counting tube was connected directly to the input amplifying circuit of a Nuclear-Chicago Corporation Model 186 decade scaler. The scaler contains a sensitivity control switch which requires the input pulse to be larger than the value selected by this control in order to produce one count. The operating characteristics of the neutron counting circuit are indicated by the curves of Figure 6. An operating voltage of 2100 volts and a sensitivity of 1 MV were selected from the plots to give operation in the plateau portion of the curve. These settings were used with the counter throughout the study.

A detector shield holder was used to position the BF_3 tube over the center of the vertical collimated beam at the same position for each configuration of the shielding blocks.

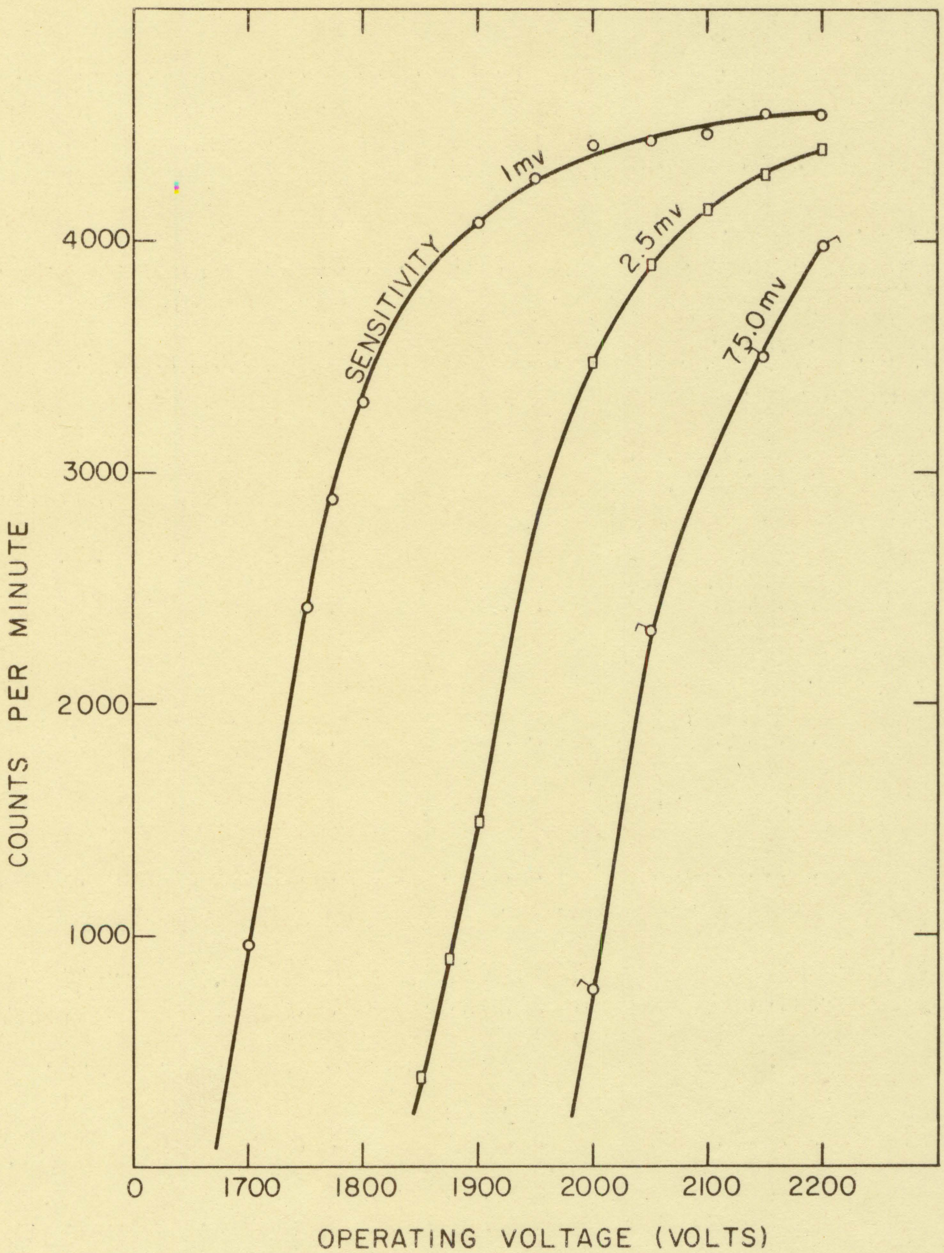

Figure 6. Operating curves for $B^{10}F_3$ lined neutron counter

It was also used to shield the tube from neutrons that had been scattered around the shield. The shielding of the detector from scattered neutrons was accomplished because the holder was filled with paraffin, and cadmium was placed around the BF_3 tube so that only neutrons entering the detector shield directly from the source through the shielding blocks would be counted, see Figure 7. Once the tube was properly positioned in the detector shield, it was sealed in with paraffin and was not removed until the study was completed.

D. Geometry

A photograph depicting the general experimental layout is shown in Figure 8. The dimensions of the apparatus and the arrangements used in the study are given in Figure 9. The shielding blocks were mounted on the source container barrel lid. The lid was fixed with small balsa wood strips so that the shielding blocks could be positioned directly over the source in the same position at every change.

The detector holder shield was positioned so that a 0.88-in. gap existed between the top of the block and the bottom of the holder. This gap allowed a cadmium strip to be inserted between the block and the detector as well as facilitating the removal of one block and allowing it to be replaced by another without removing the detector holder.

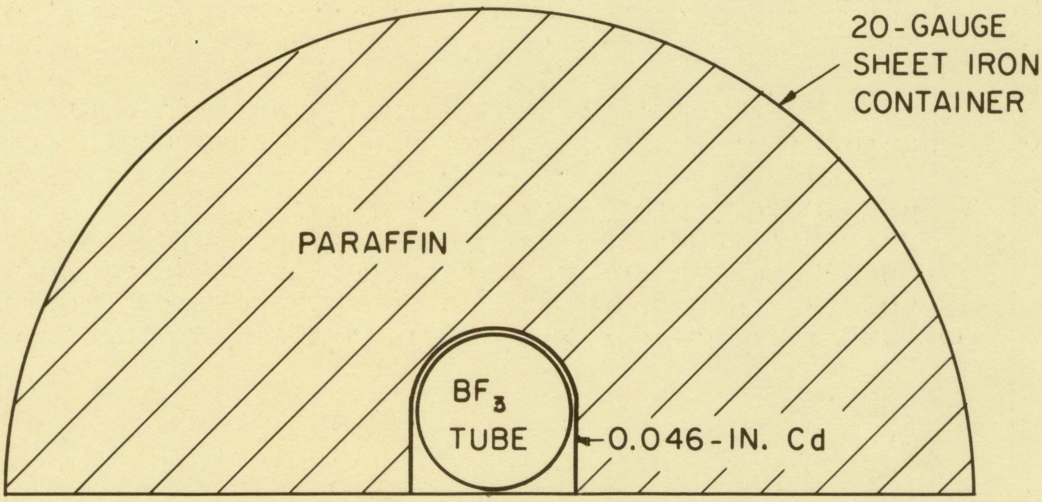

Figure 7. Cross-section of neutron detector shield

Figure 8. Experimental layout

A. Detector shield holder
B. Shielding blocks mounted on lid
C. Cadmium shrouded container barrel
D. Scaler timer
E. Decade scaler
F. Paraffin lined box

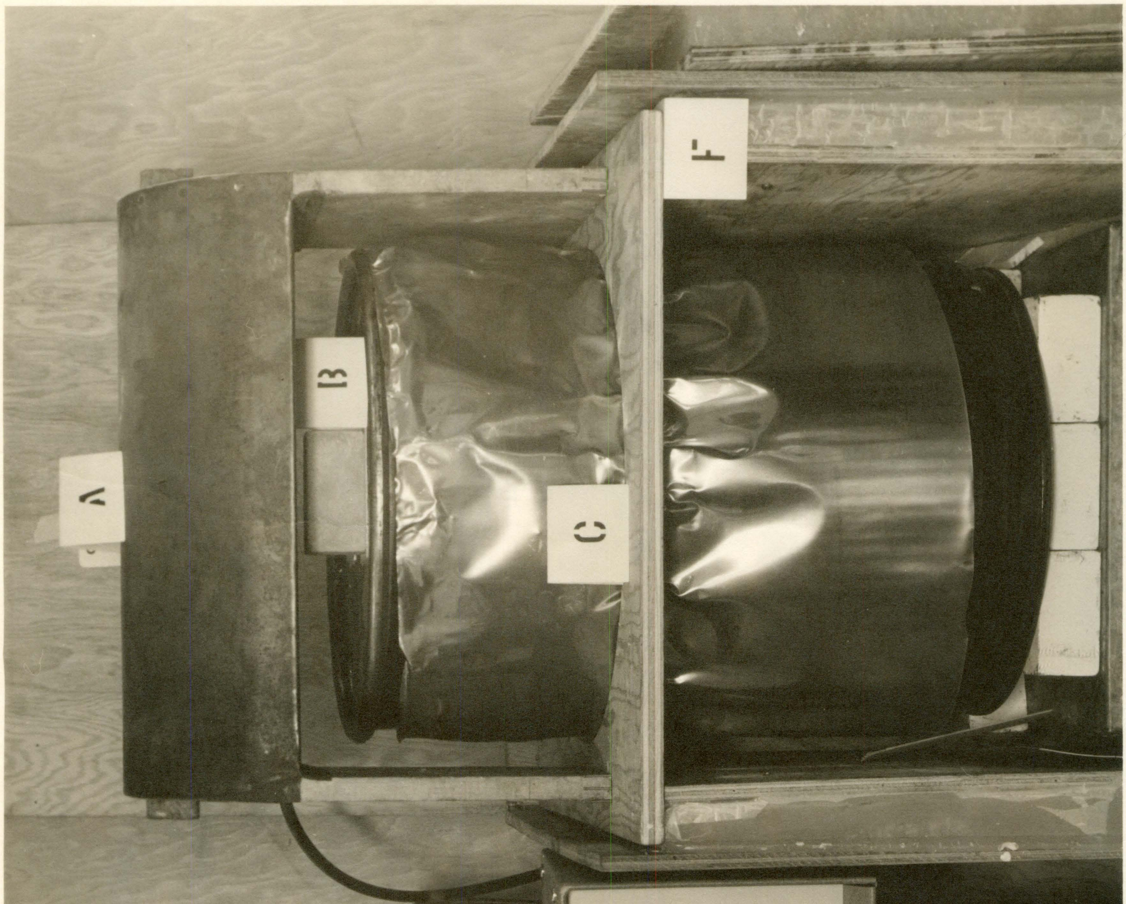
A
B
C
D
E
F

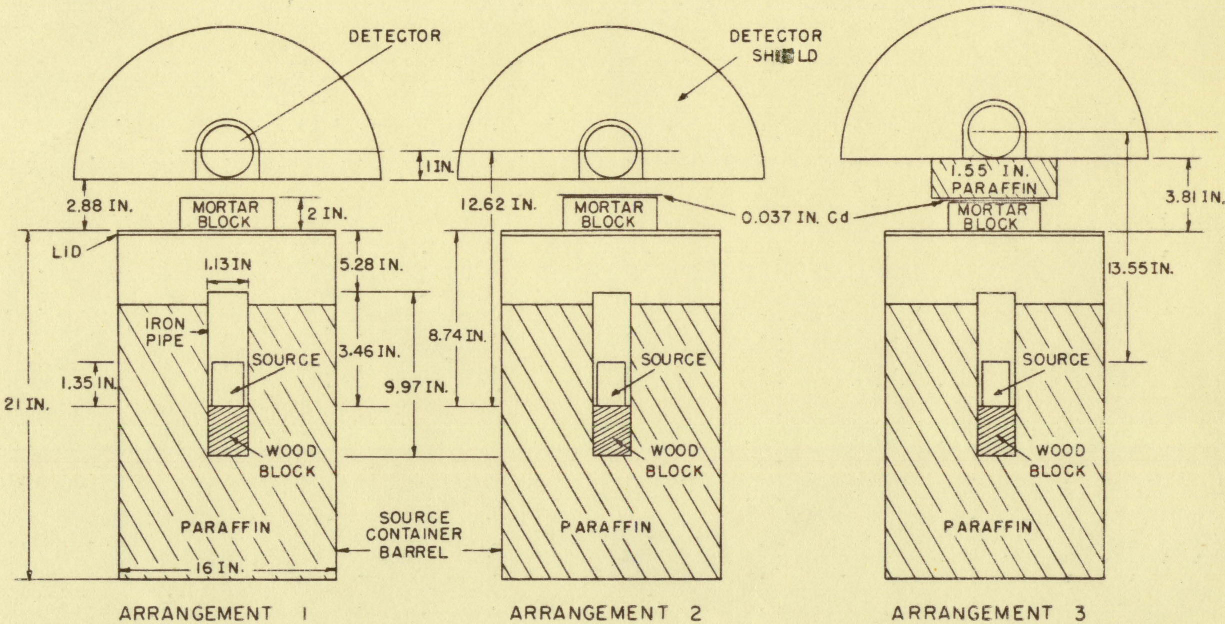

Figure 9. Experimental arrangements for neutron counting

The author was also able to change blocks from a more protected position with the use of forceps.

V. PROCEDURES

As noted before, the composition of the shielding blocks was varied for this investigation. Six different mixtures were tested in all. The composition of the six mixtures is shown in Table 3 and labeled A through I. In mixtures A through F a coarse aggregate was used. It was passed through a 3/8 in. screen but could not pass through a No. 4 screen. In mixtures G, H, and I, a fine aggregate was used. It could pass through a No. 4 screen but not through a No. 8 screen. In all the mixtures an attempt was made to keep the percentage by weight of cement and water constant, and to vary the amount of sand and aggregate but to keep the total weight percentage at a constant. An attempt was made to increase the coarse aggregate content of the blocks even more. However, the resulting blocks were so honeycombed as to render them useless for testing. The 34.36% fine aggregate mixture was also harsh and resulted in poor blocks that could not be used. The concrete blocks were able to be used with a higher aggregate content than the mortar blocks since better workability can be achieved for a given amount of water with a coarser aggregate (10, p. 52).

The procedures used for mixing and casting the blocks were the same for all mixtures. The cement and approximately one fourth of the sand and aggregate were thoroughly mixed. The sand and aggregate were both in a saturated surface dried

Table 3. Composition of mixtures

Item	Mixture								
	A	B	C	D	E	F	G	H	I
Composition (per cent by weight)									
Cement	15.60	15.60	15.35	15.60	15.60	15.60	15.60	15.35	15.60
Water	9.54	9.60	9.44	9.60	9.60	9.60	9.60	9.44	9.60
Sand	40.50	45.20	50.64	57.64	67.00	74.80	45.20	50.64	57.64
Haydite	34.36	29.60	24.57	17.16	7.80	0	29.60	24.57	17.16
Average density (gm/cm^3) Standard blocks									
7th day	2.16	2.17	2.12	2.20	2.17	2.19	2.03	2.05	2.12
28th day	2.17	2.17	2.11	2.19	2.16	2.18	2.03	2.07	2.11
Average density (gm/cm^3) Air dried blocks									
7th day	1.85	1.85	1.85	1.92	1.93	1.94	1.85	1.88	1.94
28th day	1.84	1.82	1.82	1.91	1.89	1.93	1.78	1.81	1.86

condition. Water was added, and the mixture was again mixed with a hand trowel. The remainder of the sand and aggregate was added in small amounts and mixed. After all of the sand, water, and aggregate were added to the cement, the mixing continued for several minutes to insure uniform consistency.

The machined steel mold used in casting the blocks contained twenty-four 2 by 2 by 4 inch compartments. Ten blocks were cast for mixture A and four blocks for each of the other mixtures. The compartments were filled about one third full, rodded 25 times, and filled and rodded again two more times to fill the mold. An additional portion of the mix was spread over the top and worked down with the trowel; the excess was removed leaving the mix level with the top of the mold. The mold was covered with moistened burlap and allowed to stand 24 hours. Upon removal from the mold, half of the blocks from each mixture were stored in water, and the other half were stored in the air. The temperature varied between 82 and 84°F and the relative humidity varied between 20 and 26 per cent during the period the blocks were drying. The water cured blocks will be called standard blocks while those stored in the air will be referred to as air dried blocks.

Figure 10 is a photograph showing the surface condition of some of the test blocks.

A sample of the aggregate was washed and dried at a temperature of 105°C. over night. A 24 hour water absorption

Figure 10. Photograph showing surface condition of some of the test blocks

test was then performed, and the results showed that the haydite absorbed 15.2 per cent, by weight, of the water.

The bulk specific gravity of the aggregate was next determined, using standard test methods (2, p. 1233), on a 50 KG sample in the saturated surface dry condition. A value of 1.69 was computed.

Three experimental arrangements were used to determine the relative intensity of fast and slow neutrons. The arrangements are depicted in Figure 8. Since the BF_3 tube is capable of counting neutrons of all energies to some extent, a cadmium sheet was placed on top of the block, as shown in arrangement 2, to absorb the slow neutrons (defined as neutrons of energy less than 0.025 ev). The slow neutrons were readily absorbed by the 0.037-in. of cadmium since cadmium exhibits a high neutron absorption resonance in the low energy region. It was calculated that the cadmium will capture over 99% of the incident slow neutrons. Since the readings in arrangement 1 are due to the counts recorded by the BF_3 tube for neutrons of all energies, and the readings of arrangement 2 are due to the neutrons of energies above thermal, the difference in the two is the slow neutron count.

A layer of paraffin was inserted between the cadmium and the detector in arrangement 3 to determine the fast neutron count. The paraffin, which contains a large proportion of hydrogen, slowed down part of the fast neutrons so that they could be counted by the BF_3 detector which is relatively inefficient in detecting neutrons of high energies. The paraffin also prevented those neutrons reflected and scattered from outside the shield into the detector from completely masking the relative fast neutron count. The higher counting rate also gave better counting statistics. Since the fast neutron counts were taken under a different geometry than that used to determine the slow neutron count, a correction had to be made to the fast counts so that they could be compared to the slow counts. The fast neutron counts recorded were corrected by the ratio of the squares of the distances between the source and the detector. This ratio was computed to be 1.15.

Neutron counts in all three arrangements were taken for all of the blocks on both the 7th and 28th day after they were cast. Each of the five air dried blocks of mixture A was soaked a different length of time, from five minutes to 24 hours, before the seven day test, so that the counts could be recorded as a function of the absorbed water. For the 28 day test, however, in order to get a better correlation, it was decided to soak all of the five blocks from one minute to 24 hours and to remove the blocks at different time increments, determine the neutron counts, and return them for further soaking.

The weight of the absorbed water in the standard and water soaked air dried blocks of mixture A was determined by recording the weight of each block prior to the counts being taken and subtracting from this weight a new weight taken after the block was allowed to dry for a two week period following the tests.

The volume of all the blocks was considered to be constant. After determining the weight, the density of each mixture for both the standard and air dried condition was computed in gm/cm^3.

During the testing, the detector was removed from the area near the source and a background count was taken. All counting data were corrected for the background.

Since the maximum counting rate obtained in the testing was 4750 counts per minute, no correction was deemed necessary for counter dead time.

Since the standard blocks were prone to lose their absorbed water by evaporation if kept in the air for any length of time, the counting time was kept at five minutes for each arrangement to keep the evaporation at a minimum and to still yield good statistics. The standard blocks and the blocks used in the water absorption tests were all surface blotted before being counted.

The compressive strength of the blocks was determined 80 days after casting. Two blocks from each mixture were loaded in compression along the four inch length of the blocks. The average compressive strengths of the two blocks for each mixture are reported in the Appendix. The standard blocks were returned to the water tank several hours before the compressive strength tests were conducted so that the blocks might regain most of the water they had lost.

A test was conducted to determine the effect of orientation of the block on the counting rate. Two air dried blocks, one of mortar and one of concrete, were selected at random and the counting rates were determined in their normal configurations, through the two inch thicknesses of the blocks. The blocks were then rotated about the four inch axis and the counting rate was determined for each of the other three positions. The counting rates, shown in the Appendix, indicate that with two exceptions in each block, the deviation between the counting rates was less than the standard deviation. The exceptions for the mortar deviated from the average counting rate by .765 and .989 per cent, and for the concrete, the deviation was .877 and .670 per cent.

Another test was conducted to determine the reproducibility of the counting rate in removing and replacing the detector holder. The test was conducted for the configurations of arrangements 1 and 3. The data shown in the Appendix indicate that for four runs in each configuration the deviation did not exceed the standard deviation.

A plastic 2 by 2 by 4 inch mold was constructed, filled with water, and frozen, so that the counts on the resulting ice block could be compared to the concrete and mortar blocks. The same mold was also used to cast a paraffin block which was also compared. The test results are recorded in the Appendix.

VI. RESULTS AND DISCUSSION

A. Effects of Changing Aggregate Content

The neutron counts taken for the 7-day and 28-day tests for the standard and air dried blocks of different mixtures are tabulated for the three arrangements in Tables 4 and 5. These counts were analyzed and separated into fast and slow neutron counts as shown in Tables 6 and 7. Plots of these counts are made for the concrete and mortar blocks in Figures 11 through 18.

It can be seen from these curves that the standard blocks are more effective in attenuating slow and fast neutrons than the air dried blocks. It was found, on the average, that the standard blocks were 24.5 per cent more effective than the air dried blocks in slow neutron attenuation, and 6.4 per cent more effective in fast neutron attenuation.

The standard concrete blocks were found to be slightly more effective in attenuating the neutrons than the standard mortar blocks. The concrete was, on the average, 4.5 per cent more effective in attenuating slow neutrons and 1.1 per cent more effective in attenuating fast neutrons.

The reason the standard blocks exhibit better neutron attenuation properties than the air dried blocks is due to the large amount of water absorbed in the standard blocks, see Tables 6 and 7. It can also be seen that the standard

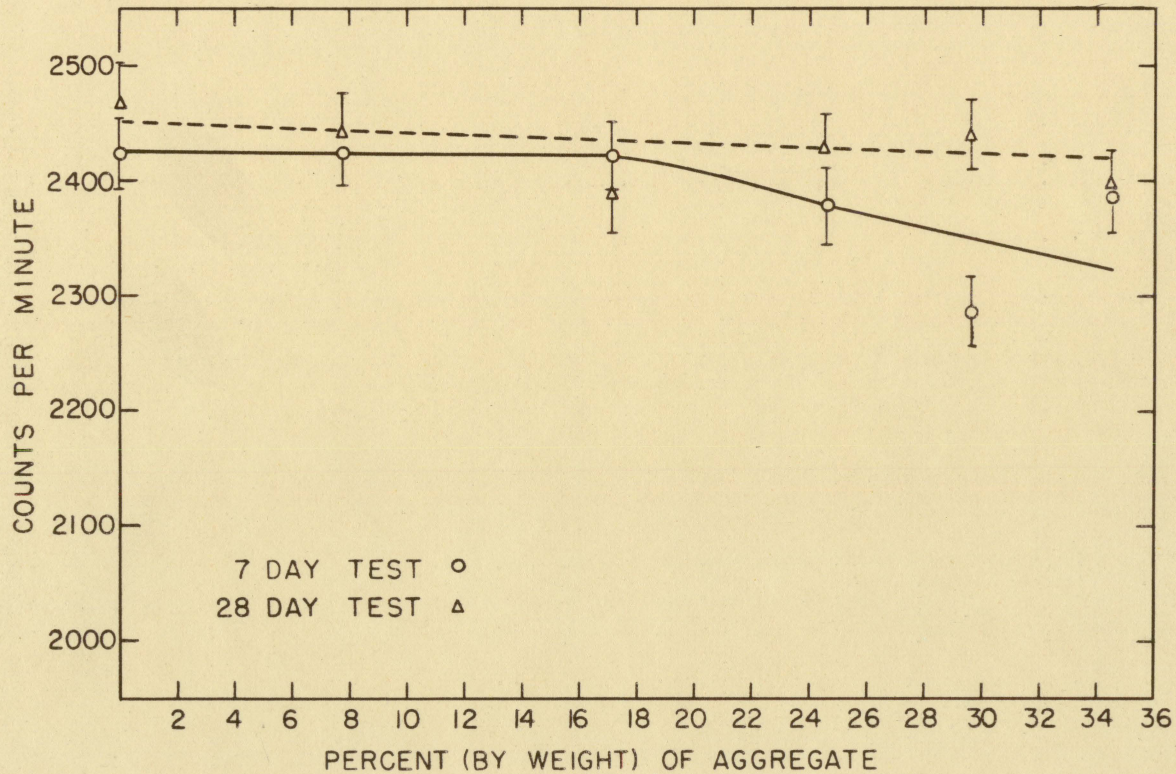

Figure 11. Slow neutron counts for standard concrete blocks

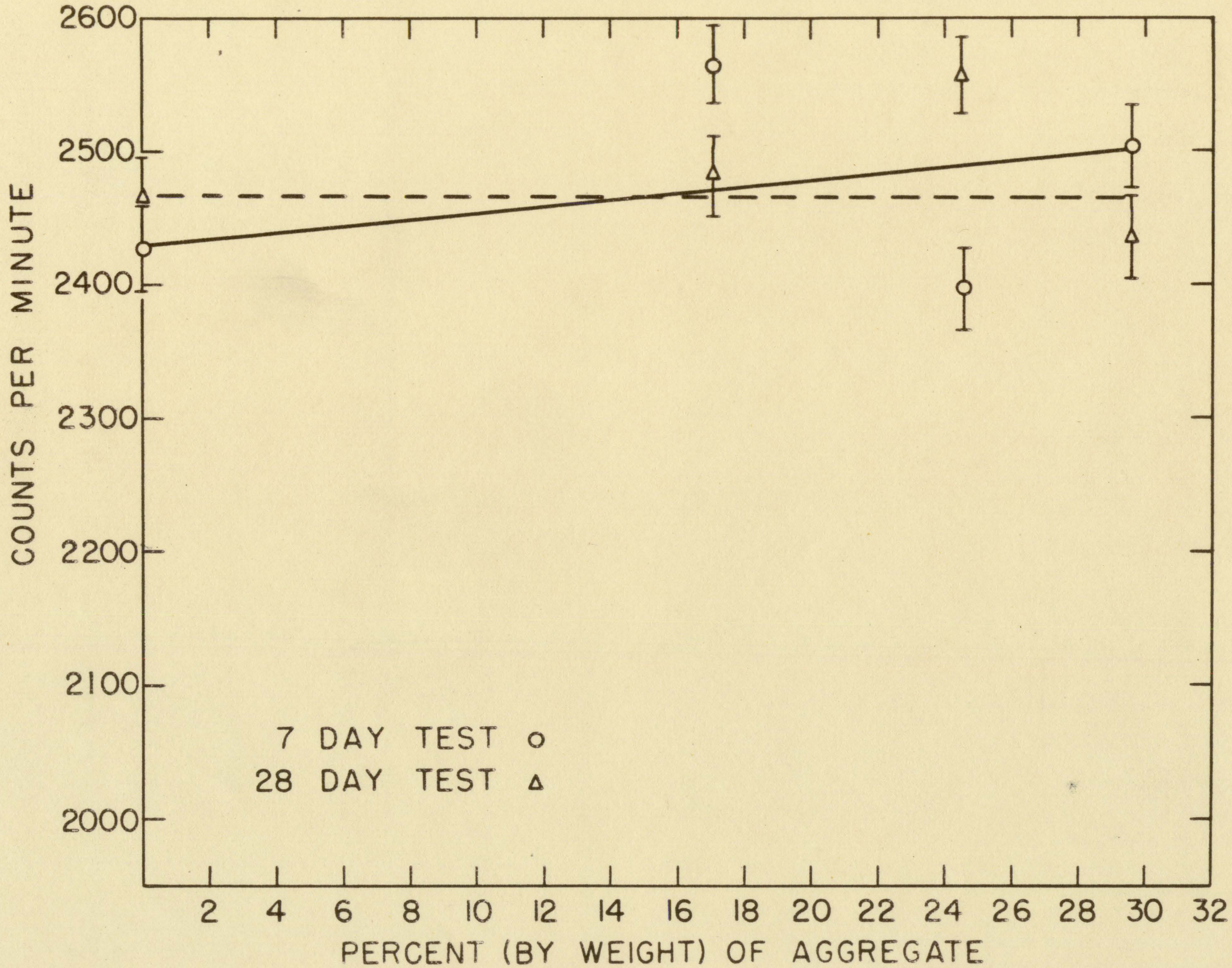

Figure 12. Slow neutron counts for standard mortar blocks

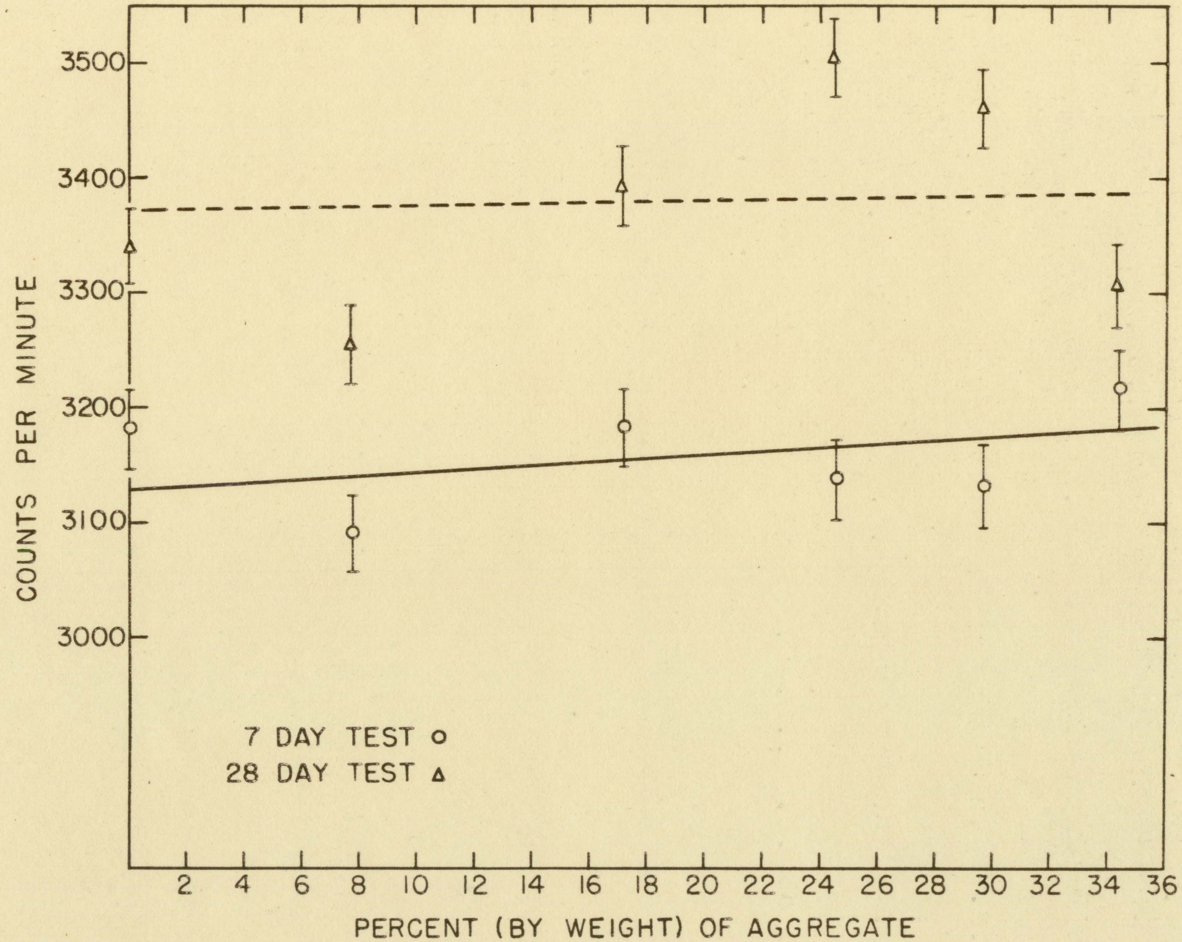

Figure 13. Slow neutron counts for air dried concrete blocks

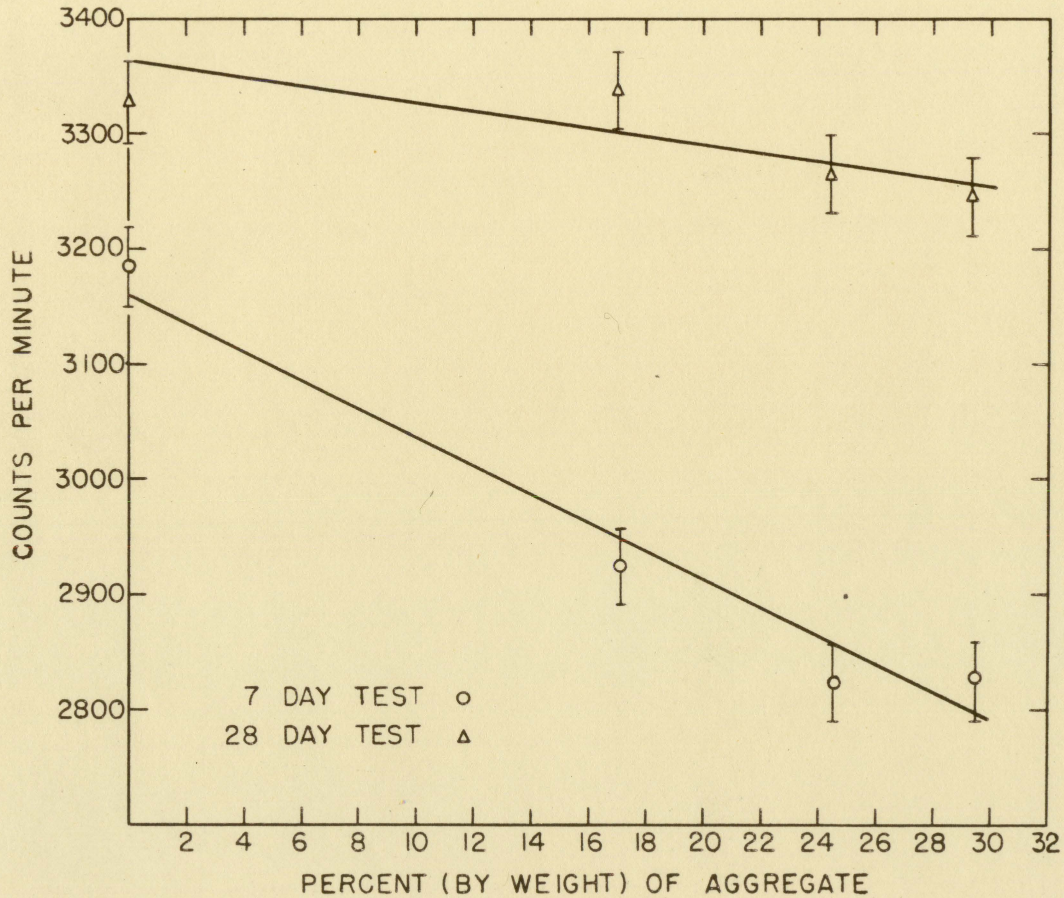

Figure 14. Slow neutron counts for air dried mortar blocks

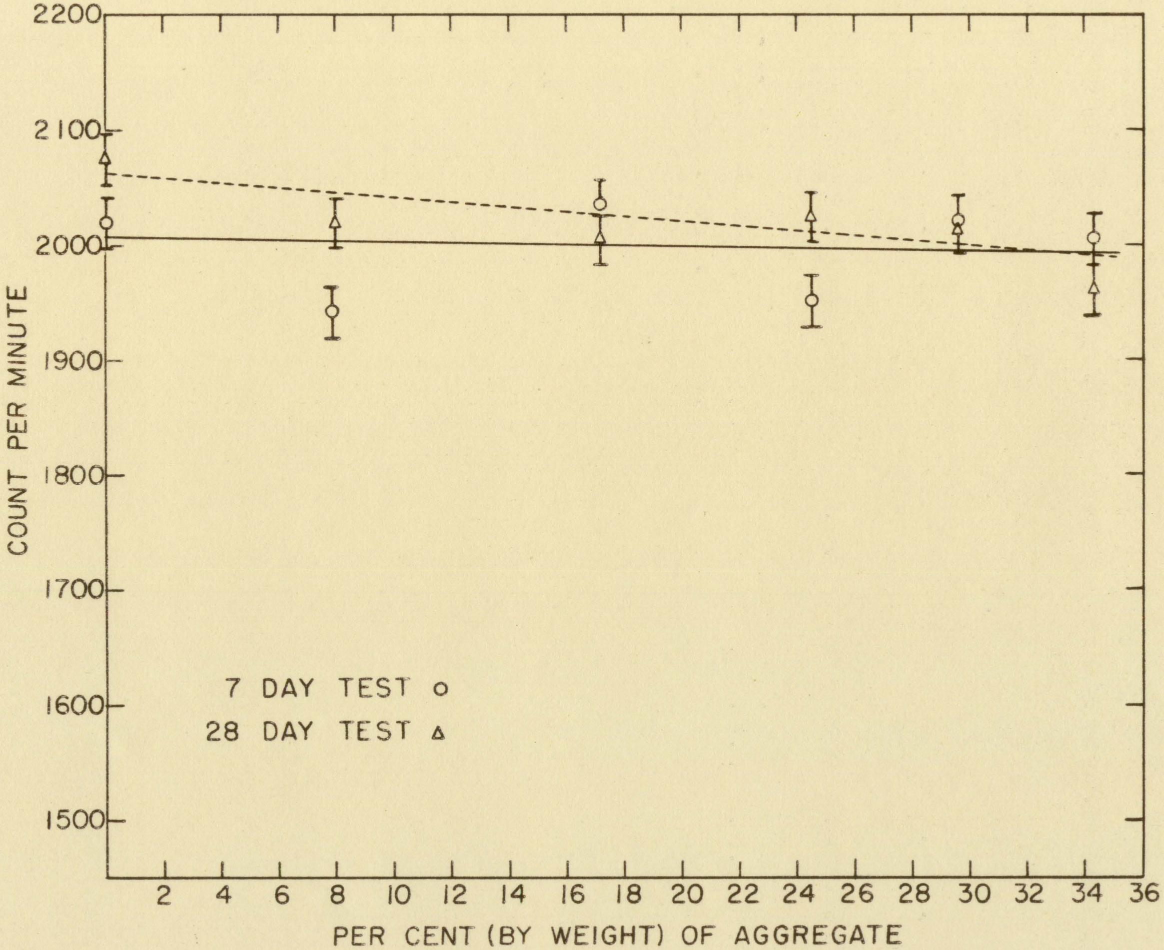

Figure 15. Fast neutron counts for standard concrete blocks

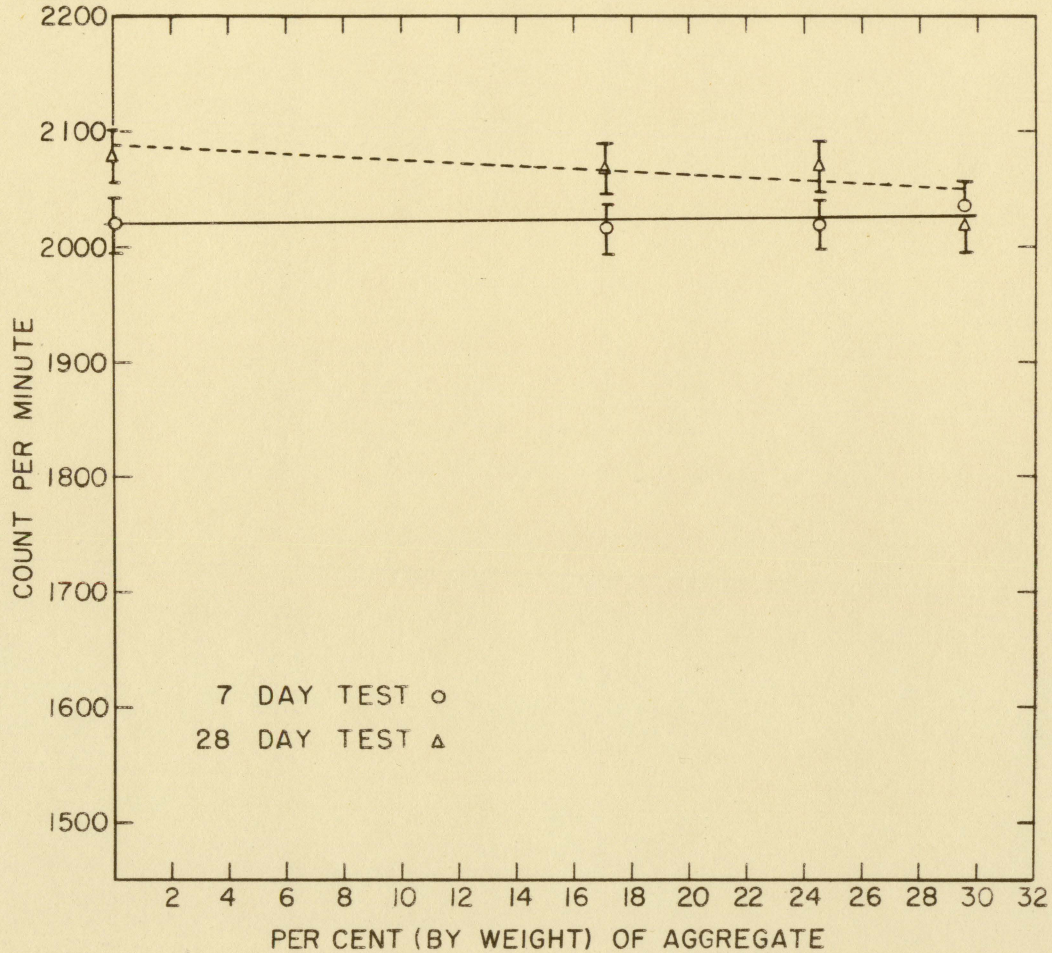

Figure 16. Fast neutron counts for standard mortar blocks

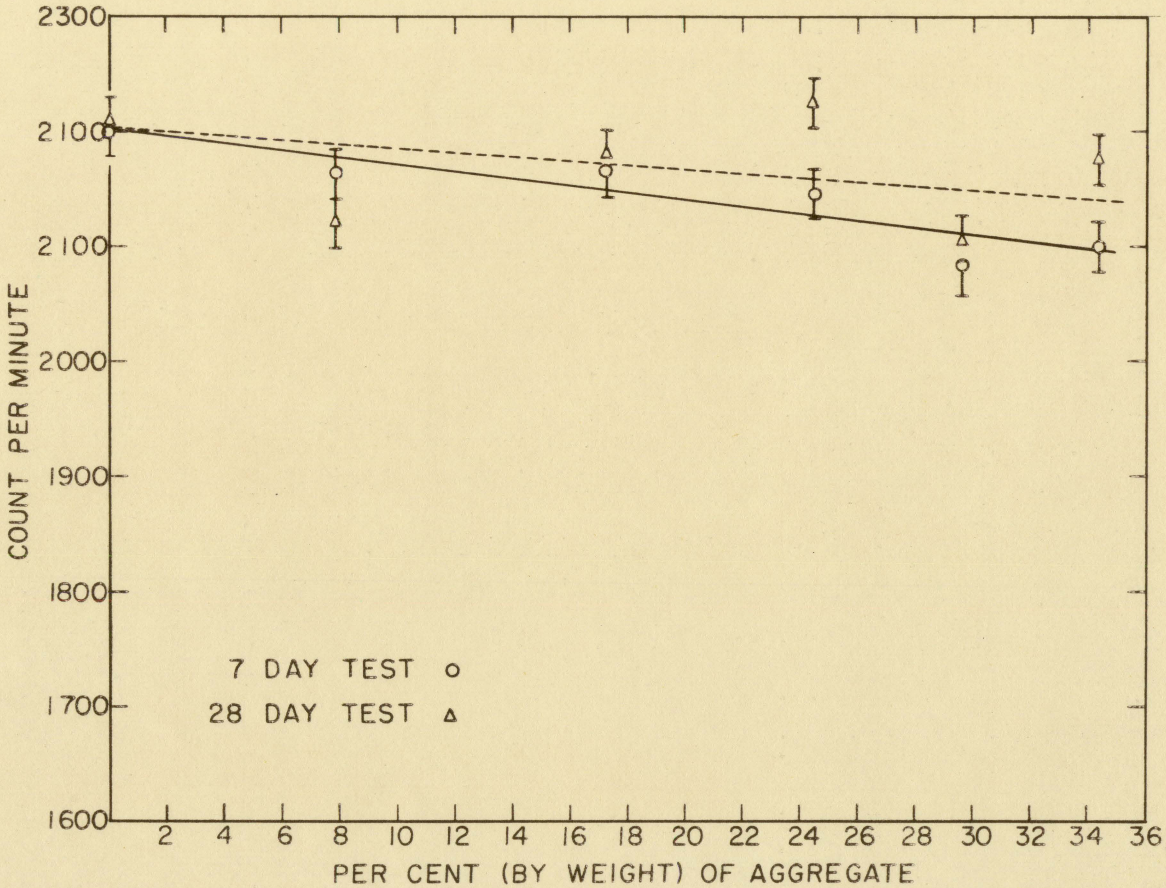

Figure 17. Fast neutron counts for air dried concrete blocks

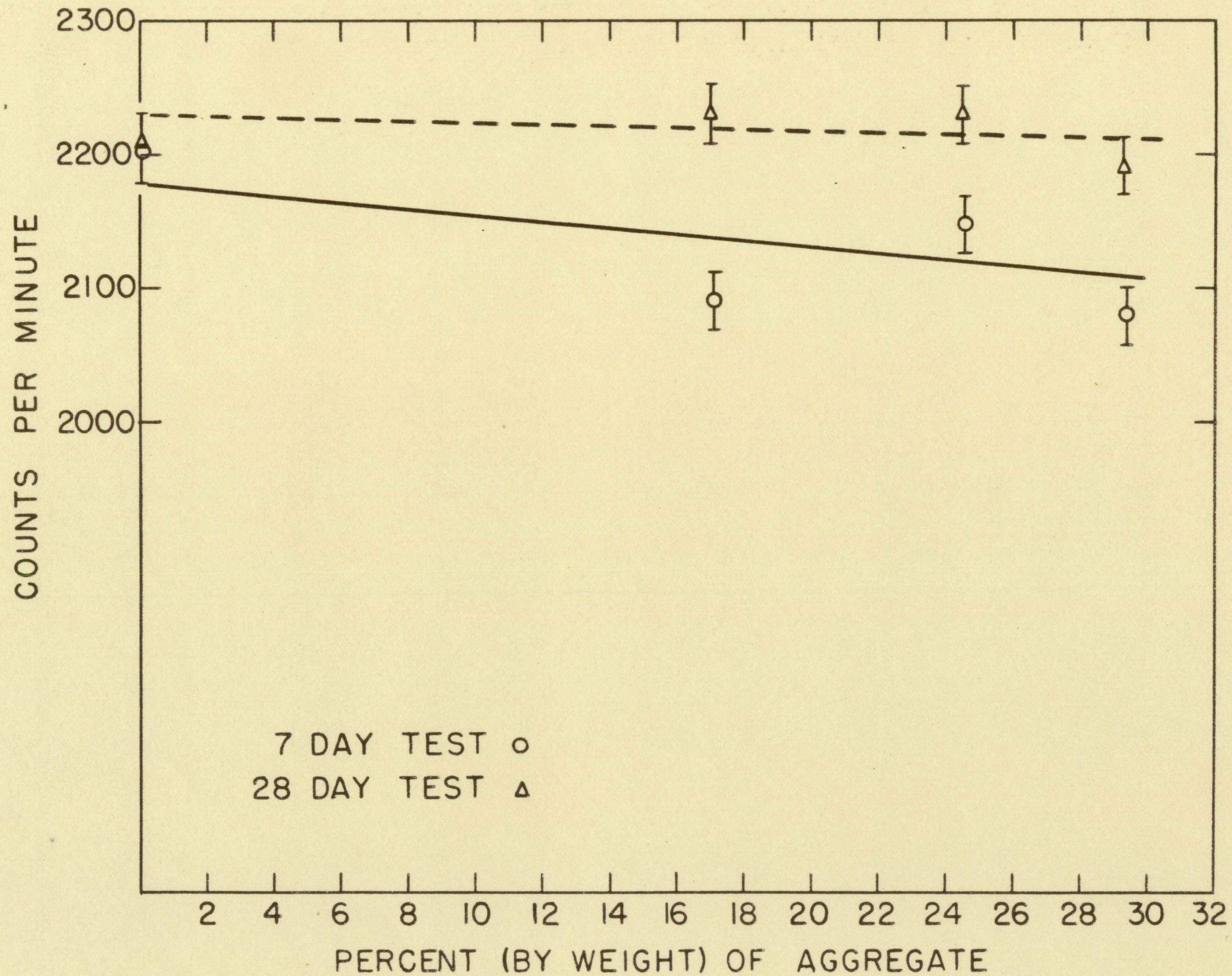

Figure 18. Fast neutron counts for air dried mortar blocks

Table 4. 7 day test data

Mixture	Arrangement	Counts	Time min.	Counting rate (R)
Background		7198	67	107 ± 1
Standard				
A	1	18053	5	3504 ± 27
B	1	17546	5	3402 ± 27
C	1	18021	5	3497 ± 27
D	1	17629	5	3419 ± 27
E	1	18265	5	3546 ± 27
F	1	18579	5	3609 ± 27
G	1	18481	5	3589 ± 27
H	1	18184	5	3530 ± 27
I	1	18837	5	3660 ± 27
A	2	6134	5	1120 ± 16
B	2	6126	5	1118 ± 16
C	2	6135	5	1120 ± 16
D	2	6019	5	1097 ± 16
E	2	6044	5	1102 ± 16
F	2	7471	5	1187 ± 16
G	2	5969	5	1087 ± 15
H	2	6205	5	1134 ± 16
I	2	6032	5	1099 ± 15
A	3	9249	5	1743 ± 19
B	3	9291	5	1751 ± 19
C	3	9899	5	1693 ± 19
D	3	9374	5	1768 ± 19
E	3	8956	5	1684 ± 19
F	3	9325	5	1758 ± 19
G	3	9381	5	1769 ± 19
H	3	9286	5	1752 ± 19
I	3	9360	5	1765 ± 19
Air dried				
A	1	22103	5	4314 ± 30
B	1	21844	5	4262 ± 30
C	1	21736	5	4240 ± 30
D	1	22325	5	4358 ± 30
E	1	21926	5	4278 ± 30
F	1	22731	5	4439 ± 30
G	1	20279	5	3949 ± 28
H	1	20546	5	4002 ± 28
I	1	20829	5	4059 ± 29
A	2	6014	5	1096 ± 16
B	2	6181	5	1129 ± 16

Table 4. (Continued)

Mixture	Arrangement	Counts	Time min.	Counting rate (R)
C	2	6042	5	1101 ± 16
D	2	6406	5	1174 ± 16
E	2	6465	5	1186 ± 16
F	2	6809	5	1255 ± 16
G	2	8811	5	1122 ± 15
H	2	6434	5	1180 ± 16
I	2	6216	5	1136 ± 16
A	3	9660	5	1825 ± 20
B	3	9584	5	1810 ± 20
C	3	9861	5	1865 ± 20
D	3	9939	5	1881 ± 20
E	3	9936	5	1880 ± 20
F	3	10101	5	1913 ± 20
G	3	9573	5	1808 ± 19
H	3	9869	5	1867 ± 20
I	3	9620	5	1817 ± 19

Table 5. 28 day test data

Mixture	Arrangement	Counts	Time min.	Counting rate (R)
Background		3242	60	54 ± 1
Standard				
A	1	17848	5	3516 ± 27
B	1	18054	5	3557 ± 27
C	1	18245	5	3595 ± 27
D	1	18237	5	3594 ± 27
E	1	17969	5	3540 ± 27
F	1	18615	5	3669 ± 27
G	1	17946	5	3535 ± 27
H	1	18195	5	3585 ± 27
I	1	18253	5	3597 ± 27
A	2	5869	5	1120 ± 15
B	2	5855	5	1117 ± 15
C	2	6099	5	1166 ± 16
D	2	6299	5	1206 ± 15
E	2	5754	5	1097 ± 15
F	2	6285	5	1203 ± 16
G	2	5770	5	1100 ± 15

Table 5. (Continued)

Mixture	Arrangement	Counts	Time min.	Counting rate (R)
H	2	5412	5	1028 ± 15
I	2	5845	5	1115 ± 15
A	3	8801	5	1706 ± 19
B	3	9028	5	1752 ± 19
C	3	9089	5	1764 ± 19
D	3	8996	5	1745 ± 19
E	3	9052	5	1756 ± 19
F	3	9309	5	1808 ± 19
G	3	9044	5	1755 ± 19
H	3	9295	5	1805 ± 19
I	3	9260	5	1798 ± 19
Air dried				
A	1	22324	5	4421 ± 30
B	1	23405	5	4627 ± 30
C	1	24030	5	4752 ± 31
D	1	22898	5	4526 ± 30
E	1	22775	5	4501 ± 30
F	1	23087	5	4563 ± 30
G	1	22569	5	4460 ± 30
H	1	22353	5	4417 ± 30
I	1	22465	5	4439 ± 30
A	2	5835	5	1113 ± 15
B	2	6101	5	1166 ± 16
C	2	6512	5	1248 ± 16
D	2	5935	5	1133 ± 15
E	2	6501	5	1246 ± 16
F	2	6446	5	1235 ± 16
G	2	6344	5	1215 ± 16
H	2	6035	5	1153 ± 15
I	2	5777	5	1101 ± 15
A	3	9691	5	1884 ± 20
B	3	9451	5	1836 ± 19
C	3	9954	5	1937 ± 20
D	3	9736	5	1893 ± 20
E	3	9481	5	1842 ± 19
F	3	9869	5	1920 ± 20
G	3	9804	5	1907 ± 20
H	3	9961	5	1938 ± 20
I	3	9964	5	1939 ± 20

Table 6. 7 day slow and fast neutron counts

Mixture	Per cent by weight of absorbed water	Slow neutron counting rate $(R_1-R_2 \pm \sqrt{\sigma_1^2+\sigma_2^2})^a$	Fast neutron counting rate $(1.15 \times R_3)^a$
Standard			
A	18.2	2384 ± 31	2005 ± 22
B	18.4	2284 ± 31	2020 ± 22
C	14.4	2377 ± 31	1950 ± 22
D	15.8	2422 ± 31	2035 ± 22
E	14.0	2444 ± 31	1940 ± 22
F	12.9	2422 ± 31	2020 ± 22
G	18.3	2502 ± 31	2037 ± 22
H	13.6	2396 ± 31	2018 ± 22
I	14.0	2561 ± 31	2030 ± 22
Air dried			
A		3218 ± 34	2100 ± 22
B		3133 ± 34	2083 ± 22
C		3139 ± 34	2145 ± 22
D		3184 ± 34	2165 ± 22
E		3092 ± 34	2164 ± 22
F		3184 ± 34	2200 ± 22
G		2827 ± 32	2079 ± 22
H		2822 ± 33	2149 ± 22
I		2923 ± 33	2091 ± 22

[a]Subscripts refer to the arrangements in Figure 8.

$\sigma = \sqrt{\frac{\text{counts}}{\text{time in minutes}}}$.

concrete blocks absorbed slightly more water than the standard mortar blocks, and they will, therefore, be more effective than the mortar blocks.

The curves indicate that in the standard blocks there is little increase in neutron attenuation as the aggregate content is increased. The small negative slopes of Figures 9, 14 and 15 are due to the increased water content of the

Table 7. 28 day slow and fast neutron counts

Mixture	Per cent by weight of absorbed water	Slow neutron counting rate $(R_1-R_2\pm\sqrt{\sigma_1^2+\sigma_2^2})$[a]	Fast neutron counting rate $(1.15 \times R_3)$[a]
Standard			
A	18.2	2396 ± 31	1960 ± 22
B	18.4	2440 ± 31	2015 ± 22
C	14.4	2429 ± 31	2025 ± 22
D	15.4	2388 ± 31	2005 ± 22
E	13.1	2443 ± 31	2020 ± 22
F	10.9	2466 ± 31	2078 ± 22
G	18.1	2435 ± 31	2019 ± 22
H	14.3	2557 ± 31	2070 ± 22
I	14.0	2482 ± 31	2068 ± 22
Air dried			
A		3308 ± 34	2176 ± 23
B		3461 ± 34	2110 ± 22
C		3504 ± 34	2225 ± 23
D		3393 ± 34	2180 ± 23
E		3255 ± 34	2120 ± 22
F		3328 ± 34	2208 ± 23
G		3245 ± 34	2191 ± 23
H		3264 ± 34	2230 ± 23
I		3338 ± 34	2231 ± 23

[a]Subscripts refer to the arrangements in Figure 8. $\sigma = \sqrt{\frac{\text{counts}}{\text{time in minutes}}}$.

blocks at the higher aggregate content.

The scattering of the points on the plots is due to the large statistical deviations resulting from the short duration of the counting time.

The air dried mortar blocks are seen to have a larger shielding effectiveness than the air dried concrete blocks. The reason being that for a given cement content, the larger the aggregate size, the lower the water requirements, so each mortar block will contain more water than the comparable concrete block and attenuate the neutrons more effectively. The count rate for the 7 day test was in all cases lower than the rates for the twenty eight day tests in the air dried blocks. This was due to the loss of water by evaporation in the twenty one day increment between tests. A larger percentage of water will evaporate for a given length of time in the mortar blocks, again due to the larger surface area of the fine aggregate; consequently, the curves of Figures 13 and 17 are separated a greater distance than the curves of Figures 12 and 16 at the higher aggregate contents.

It can be shown, by utilization of the removal cross section concept, why there was such a small gain in fast neutron attenuation effectiveness in using the standard concrete blocks, containing high percentages of haydite aggregate, compared to the concrete blocks of the mixture without the aggregate. Goldstein (8, p. 265) states that a corollary of the removal cross section concept is that the removal cross sections of materials mixed together are additive. This property was used by Price and Horton (12, p. 262) and by Blizzard and Miller (3, p. 22) in calculating the average fast neutron relaxation length, λ_r, for different concretes. The length for a typical ordinary Portland concrete with density of 2.3 gm/cm^3 was computed to be 10.6 cm by Price, and a length of 11.3 cm was calculated by Blizzard for dry ordinary concrete with density equal to 2.39 gm/cm^3.

With the values for the chemical composition of the Portland cement and haydite aggregate listed in Table 1 assumed correct, and with the further assumption that the composition of the sand used in the blocks was 75 per cent SiO_2 and 25 per cent $K\,Al\,Si_3\,O_4$, a value for Σ_r/ρ was computed for an air dried block of mixture A in Table 8. This value, times the density of the block, will yield $_r$:

$$\Sigma_r = \Sigma_r/\rho \times \rho = .03816 \times 1.84 = .0702\ cm^{-1}$$

and

$$\lambda_r = 1/\Sigma_r = 1/.0702 = 14.2\ cm\ .$$

Table 8. Determination of Σ_r/ρ for a dry concrete of mixture A

Element	Concentration (wt.%)	Σ_r/ρ (cm^2/g)[a]	wt.% Σ_r/ρ (cm^2/g)
H	1.05	5.98×10^{-2}	$.627 \times 10^{-2}$
O	42.49	3.72×10^{-2}	1.580×10^{-2}
Si	36.30	3.01×10^{-2}	1.092×10^{-2}
Al	4.88	2.92×10^{-2}	$.143 \times 10^{-2}$
Fe	.44	2.14×10^{-2}	$.009 \times 10^{-2}$
Ca	12.88	2.43×10^{-2}	$.312 \times 10^{-2}$
Mg	.19	3.33×10^{-2}	$.006 \times 10^{-2}$
K	1.9	2.47×10^{-2}	$.047 \times 10^{-2}$
		Total	3.816×10^{-2}

[a]Blizzard and Miller (3, p. 22).

A new value of Σ_r/ρ for the block of mixture A, after absorbing 18 per cent, by weight, water was computed on Table 9 and found to be .04758 cm^2/g. Σ_r, for the new density of 2.17 g/cm^3, will then be equal to:

$$.04758 \times 2.17 = .1033 \text{ cm}^{-1}$$

and

$$\lambda_r = 1/.1033 = 9.68 \text{ cm} .$$

Table 9. Determination of Σ_r/ρ for the concrete of mixture A with 18% absorbed water

Element	Concentration	Wt.% Σ_r/ρ (cm^2/g)
H	2.58	1.55×10^{-2}
O	49.60	1.84×10^{-2}
Si	30.77	$.93 \times 10^{-2}$
Al	4.13	$.12 \times 10^{-2}$
Fe	.37	$.008 \times 10^{-2}$
Ca	10.90	$.265 \times 10^{-2}$
Mg	.16	$.005 \times 10^{-2}$
K	1.61	$.040 \times 10^{-2}$
	Total	4.758×10^{-2}

It can now be seen that the relaxation length of 9.68 cm for Block A with 18 per cent absorbed water does not indicate much more shielding effectiveness than a typical ordinary Portland concrete block with a relaxation length of

10.6 cm.

B. Effects of Absorbed Water

The neutron counts taken for the 7 and 28 day absorbed water tests of the blocks of mixture A were tabulated on Tables 10 and 12. The analysis of the counts separated into the fast and slow neutron counts are shown on Tables 11 and 13. Plots of these counts are made for the concrete and mortar blocks in Figures 19 through 22. The slow and fast neutron count rates for the ice and paraffin blocks were also plotted on the figures.

All of the curves indicate that as the percentage of

Table 10. 7 day absorption test data

Arrangement	Absorbed water (per cent by weight)	Counts	Counting time	Net counting rate
1	0	22106	5	4207 ± 30
1	7.74	19466	5	3786 ± 28
1	8.44	19277	5	3748 ± 28
1	11.70	18416	5	3576 ± 27
1	15.40	18045	5	3498 ± 27
2	0	6015	5	1096 ± 16
2	7.74	6498	5	1193 ± 16
2	8.44	6533	5	1200 ± 16
2	11.70	6340	5	1161 ± 16
2	15.40	6024	5	1095 ± 15
3	0	9770	5	1847 ± 20
3	7.74	9510	5	1795 ± 20
3	8.44	9550	5	1803 ± 20
3	11.70	9350	5	1763 ± 19
3	15.40	9275	5	1745 ± 19

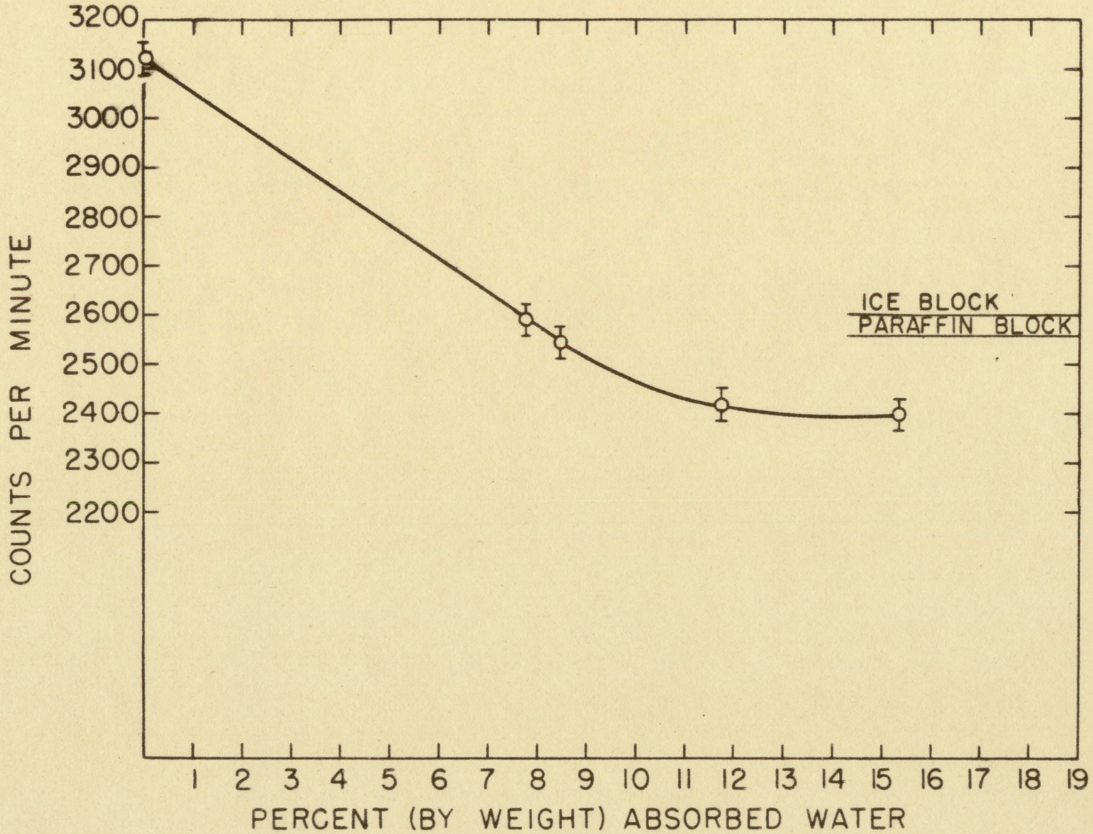

Figure 19. Slow neutron counts for 7 day water absorption test

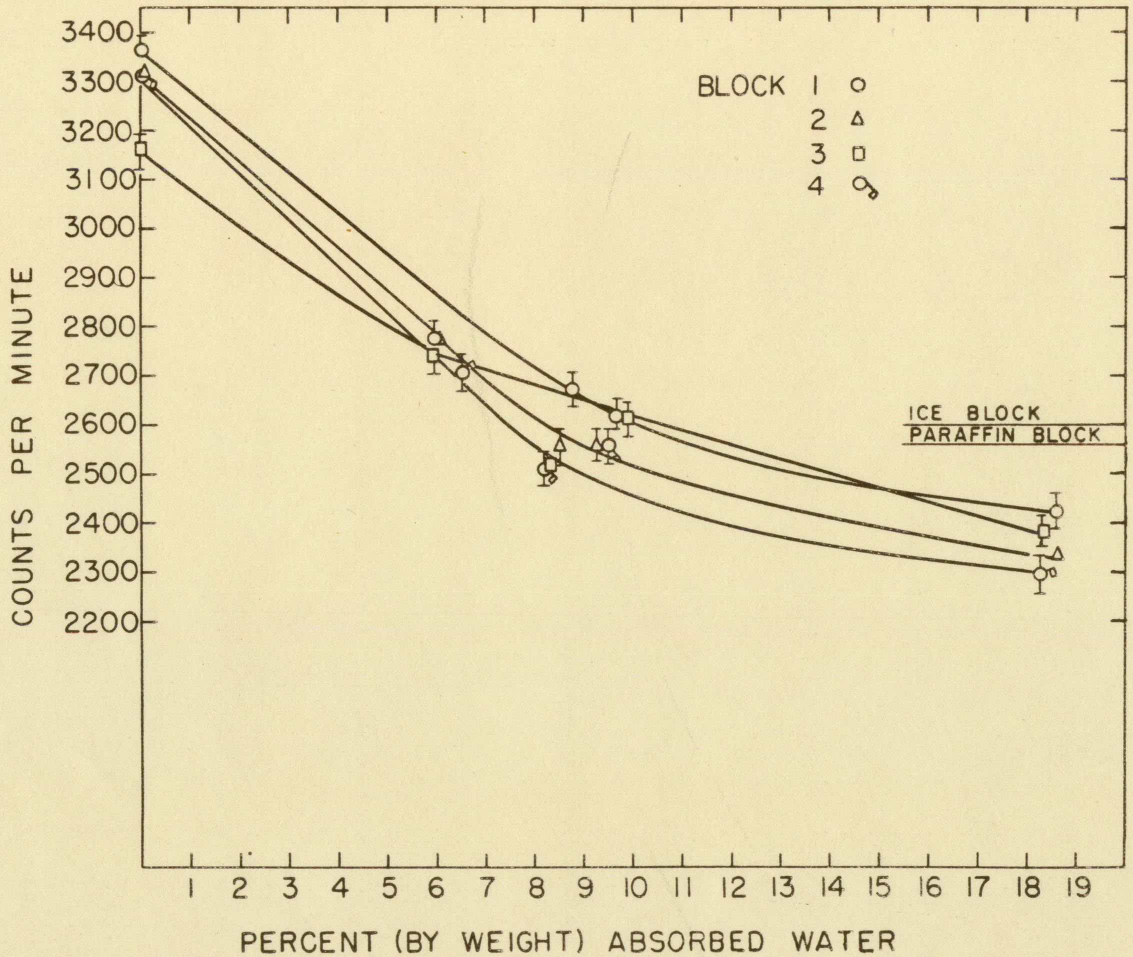

Figure 20. Slow neutron counts for 28 day water absorption test

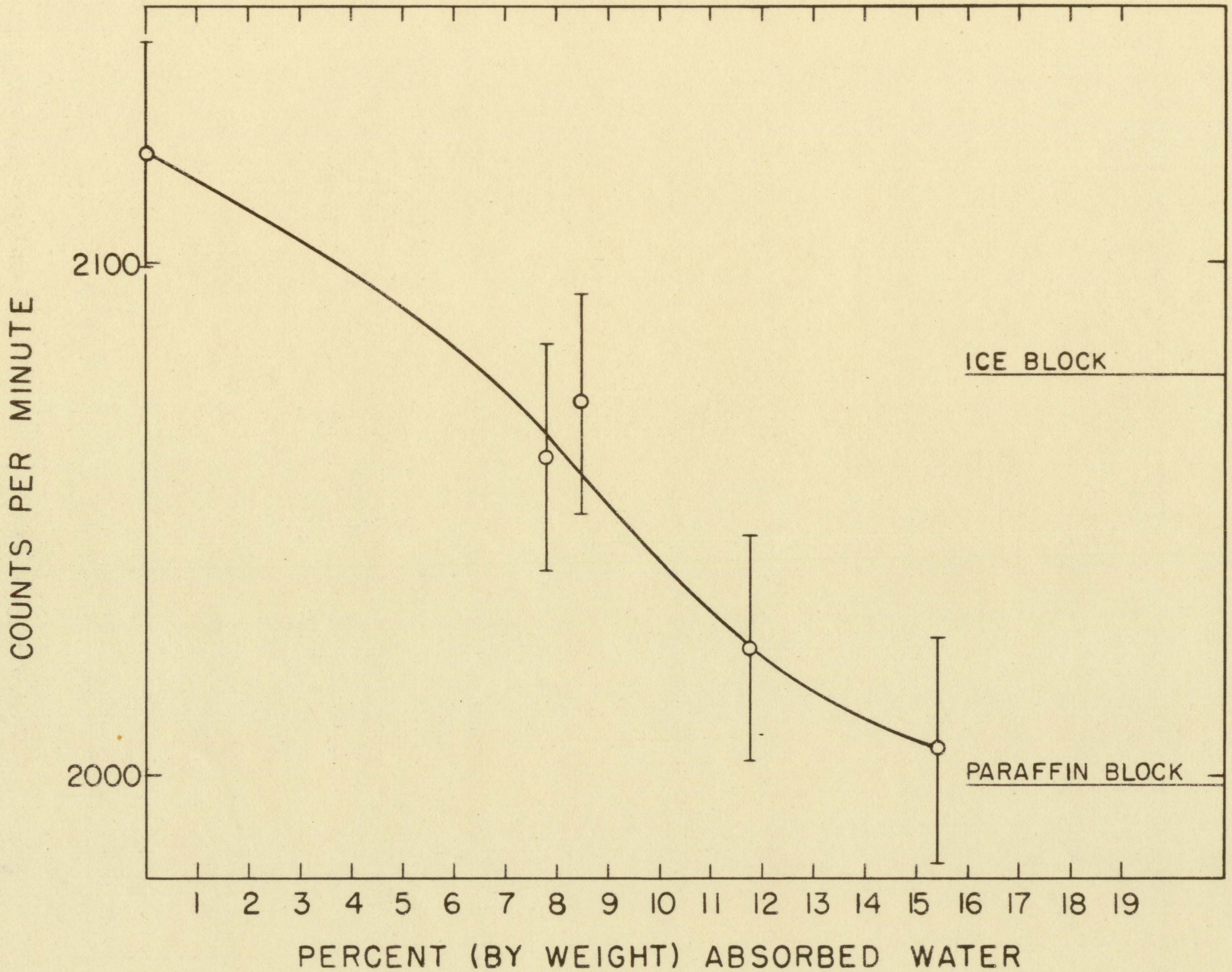

Figure 21. Fast neutron counts for 7 day water absorption test

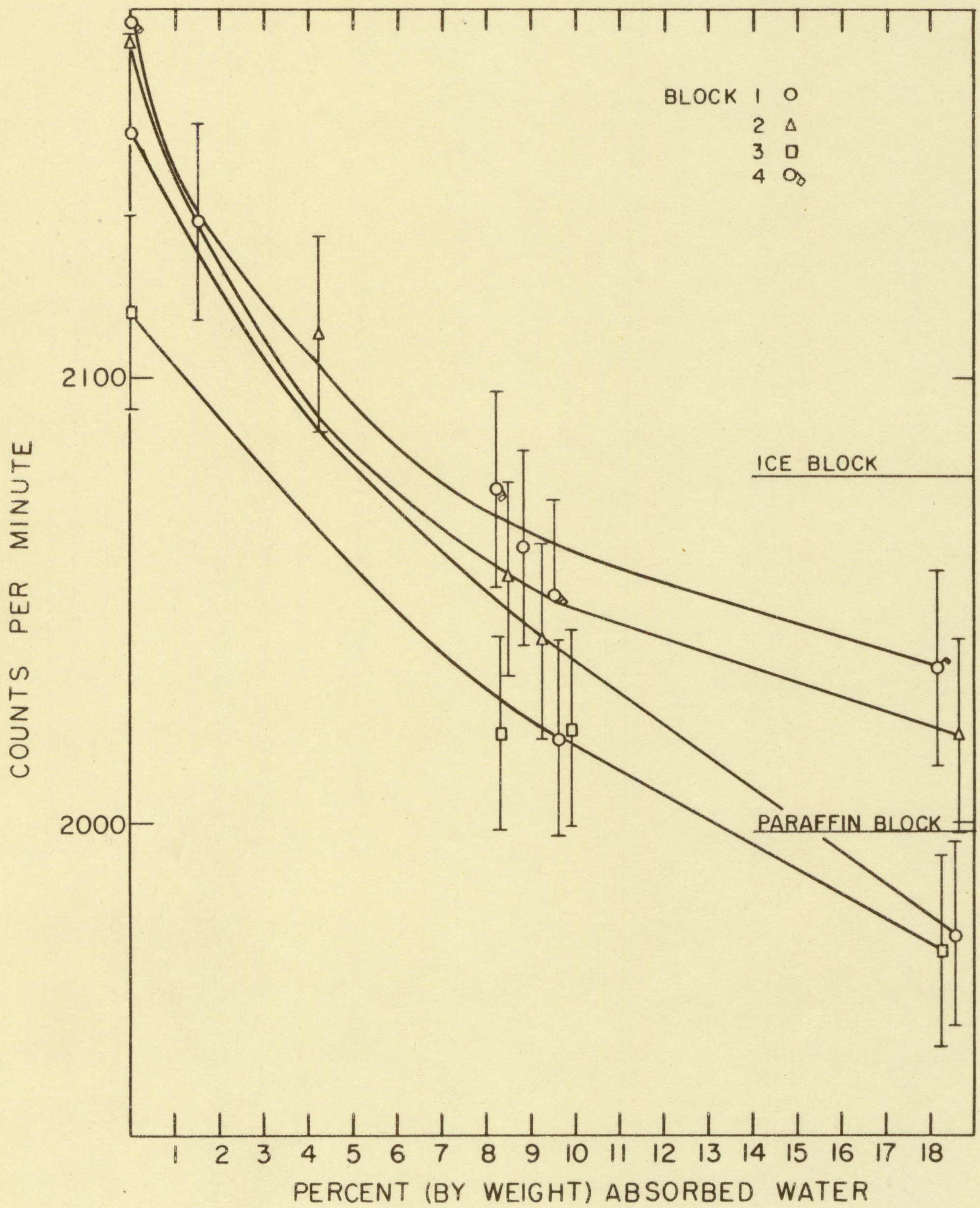

Figure 22. Fast neutron counts for 28 day water absorption test

Table 11. Slow and fast neutrons, 7 day absorption test

Absorbed water (per cent by weight)	Slow neutron counting rate	Fast neutron counting rate
0	3111 ± 34	2121 ± 23
7.74	2593 ± 32	2062 ± 23
8.44	2548 ± 32	2073 ± 22
11.70	2415 ± 32	2025 ± 22
15.40	2403 ± 31	2005 ± 22

absorbed water is increased, the neutron shielding effectiveness is also increased. A comparison of the relaxation length for the air dried block, 14.2 cm, with the length for the same block with 18 per cent absorbed water, 9.68 cm., would indicate that the trend follows the removal cross section theory.

Price (12, p. 285) states that the relaxation length for water for the fast neutron group is around 10 cm., hence, block A with 18 per cent absorbed water and the lower relaxation length of 9.68 cm. should be a bit more effective as a neutron shield than water. The count rates for the ice block shown on the curves, however, are much larger than should be expected. This can be explained by the fact that the ice block was melting during the test, losing 5 grams of weight, and, therefore, decreasing its shielding effectiveness. Also its weight prior to the test, 211.9 grams, was

Table 12. 28 day absorption test data

Block	Arrangement	Absorbed water (per cent by weight)	Counts	Counting time (min.)	Net counting rate (CPM)
1	1	0	23167	5	4538 ± 30
2	1	0	22663	5	4438 ± 30
3	1	0	22310	5	4367 ± 30
4	1	0	22578	5	4421 ± 30
1	1	5.94	20060	5	3917 ± 28
2	1	6.05	20120	5	3929 ± 28
3	1	5.90	19955	5	3896 ± 28
4	1	6.51	19319	5	3769 ± 28
1	1	8.78	19383	5	3782 ± 28
2	1	8.47	18984	5	3702 ± 28
3	1	8.29	18907	5	3687 ± 28
4	1	8.20	18655	5	3637 ± 27
1	1	9.60	19089	5	3723 ± 28
2	1	9.25	18514	5	3608 ± 27
3	1	9.87	18768	5	3659 ± 27
4	1	9.48	18574	5	3620 ± 27
1	1	18.60	17989	5	3503 ± 27
2	1	18.65	17422	5	3389 ± 26
3	1	18.35	17776	5	3460 ± 27
4	1	18.25	17721	5	3449 ± 27
1	2	0	6344	5	1174 ± 16
2	2	0	6079	5	1121 ± 16
3	2	0	6463	5	1198 ± 16
4	2	0	6039	5	1113 ± 16
1	2	5.94	6194	5	1144 ± 16
2	2	6.05	6272	5	1159 ± 16
3	2	5.90	6231	5	1151 ± 16
4	2	6.51	5778	5	1061 ± 15
1	2	8.78	5999	5	1105 ± 16
2	2	8.47	6216	5	1148 ± 16
3	2	8.29	6344	5	1174 ± 16
4	2	8.20	6108	5	1127 ± 16
1	2	9.60	5989	5	1103 ± 16
2	2	9.25	5742	5	1053 ± 15
3	2	9.87	5713	5	1048 ± 15
4	2	9.48	5798	5	1065 ± 15
1	2	18.60	5868	5	1079 ± 15
2	2	18.65	5760	5	1057 ± 15
3	2	18.35	5864	5	1078 ± 15
4	2	18.25	6249	5	1155 ± 16

Table 12. (Continued)

Block	Arrangement	Absorbed water (per cent by weight)	Counts	Counting time (min.)	Net counting rate (CPM)
1	3	0	9839	5	1871 ± 20
2	3	0	9905	5	1884 ± 20
3	3	0	9677	5	1838 ± 20
4	3	0	9961	5	1896 ± 20
1	3	1.45	9775	5	1857 ± 20
2	3	4.13	9638	5	1828 ± 20
1	3	8.78	9445	5	1793 ± 19
2	3	8.47	9432	5	1787 ± 19
3	3	8.29	9281	5	1757 ± 19
4	3	8.20	9483	5	1802 ± 19
1	3	9.60	9251	5	1754 ± 19
2	3	9.25	9368	5	1778 ± 19
3	3	9.87	9281	5	1759 ± 19
4	3	9.48	9384	5	1782 ± 19
1	3	18.60	9078	5	1718 ± 19
2	3	18.65	9276	5	1758 ± 19
3	3	18.35	9058	5	1715 ± 19
4	3	18.25	9338	5	1770 ± 19
Background			5703	60	95 ± 1

much less than that expected for a 2 by 2 by 4 inch block, which should be around 254 grams, so a valid comparison can not be made.

The fast neutron relaxation length for paraffin wax was computed to be approximately 7 cm., indicating that it should be a bit more effective as a fast neutron shield than the block with 18% water. The position of the count rate line for the paraffin on Figures 21 and 22 would tend to substantiate the calculation.

In the attenuation of slow neutrons, however, Figures

Table 13. Slow and fast neutrons 28 day water absorption test

Slow neutrons			Fast neutrons		
Block	Per cent absorbed water	Counting rate	Block	Per cent absorbed water	Counting rate
1	0	3364 ± 34	1	0	2155 ± 23
2	0	3317 ± 34	2	0	2175 ± 23
3	0	3169 ± 34	3	0	2115 ± 23
4	0	3308 ± 34	4	0	2180 ± 23
1	5.94	2773 ± 31	1	1.45	2135 ± 23
2	6.05	2770 ± 31	2	4.13	2110 ± 23
3	5.90	2745 ± 31	1	8.78	2062 ± 22
4	6.51	2708 ± 31	2	8.47	2055 ± 22
1	8.78	2677 ± 31	3	8.29	2020 ± 22
2	8.47	2554 ± 31	4	8.20	2075 ± 22
3	8.29	2513 ± 31	1	9.60	2019 ± 22
4	8.20	2510 ± 31	2	9.25	2041 ± 22
1	9.60	2620 ± 31	3	9.87	2021 ± 22
2	9.25	2555 ± 31	4	9.48	2051 ± 22
3	9.87	2611 ± 31	1	18.60	1975 ± 22
4	9.48	2555 ± 31	2	18.65	2019 ± 22
1	18.60	2424 ± 31	3	18.35	1971 ± 22
2	18.65	2332 ± 31	4	18.25	2035 ± 22
3	18.35	2382 ± 31			
4	18.25	2294 ± 31			

19 and 20 indicate that the paraffin block is not as effective as a concrete block containing over 9 per cent absorbed water.

To determine if the neutron level decreased exponentially with the addition of water, the curves were also plotted on semilog paper on Figure 23. The resulting curves show that the slow neutron attenuations may be approximated very closely by a straight line on the plot, and that the fast neutron attenuation does follow a straight line plot. The 28 day fast neutron attenuation curve was found to fit the

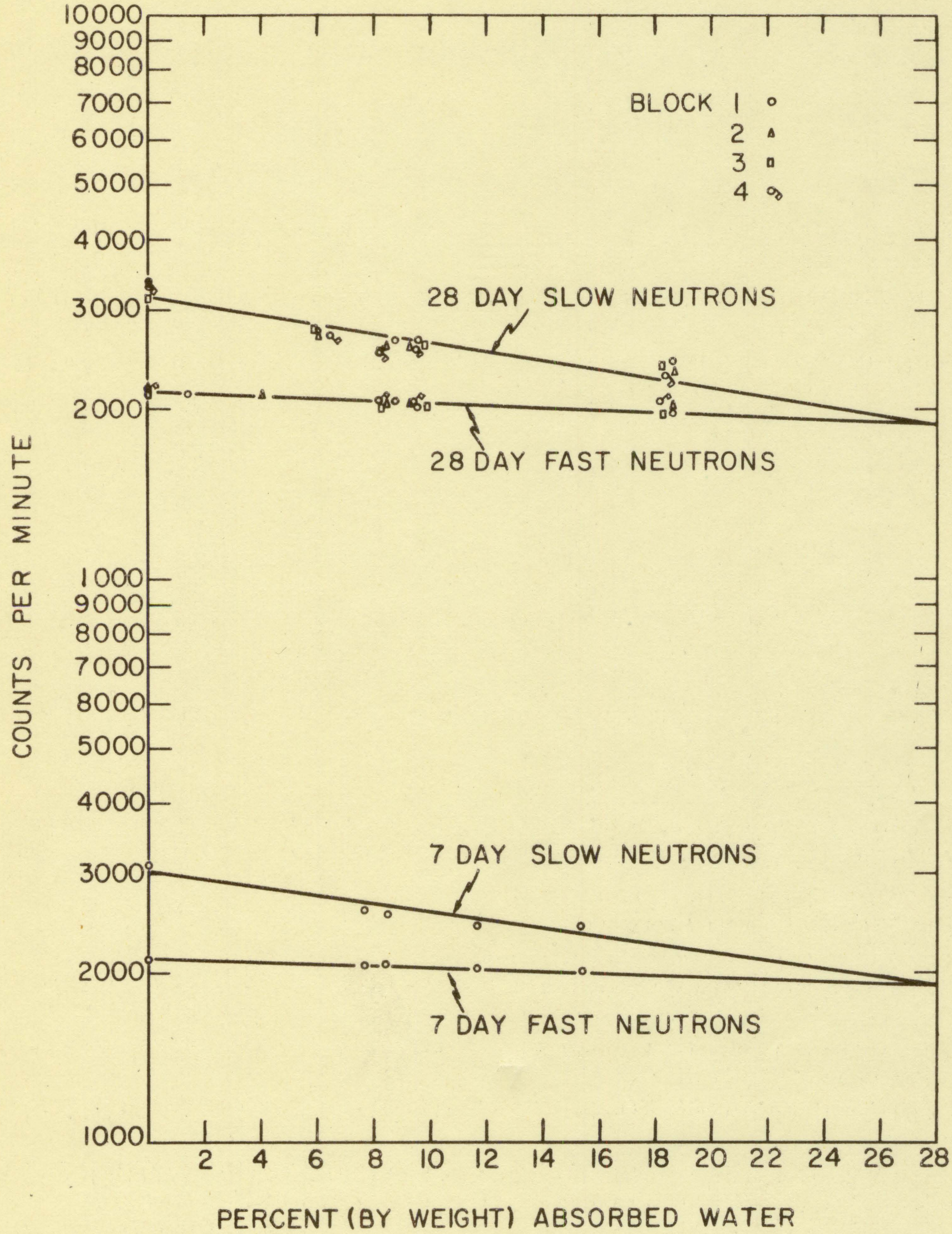

Figure 23. Neutron counts for water absorption tests

following equation:

$$y = 2150 e^{-.0049x}$$

where y is equal to the counting rate, and x is equal to the per cent of absorbed water. The 28 day slow neutron attenuation line was found to fit an equation of the following form:

$$y = 3150 e^{-.019x}$$

The addition of 18 per cent water was found to decrease the slow neutron counts 28.1 per cent, and the fast neutron counts 8.61 per cent for the twenty eight day test.

Goldstein (8, p. 99) states that a strict 1/v detector measures neutron density and not flux, and, consequently, in order to convert the readings from such a detector to flux they must be multiplied by some appropriate speed for the neutrons. Since the $B^{10}(n, \alpha)$ reaction of the detector used in this study satisfies the 1/v law, see Glasstone and Edlund (7, p. 57), the count rates for the tests of this study may be assumed proportional to the neutron flux.

VII. CONCLUSIONS

The following conclusions seem justified concerning the neutron shielding effectiveness of the mixtures and materials used under the conditions of this study.

1. There seems to be little advantage in using concretes and mortars containing high percentages of haydite aggregate over an ordinary typical Portland concrete in neutron shielding effectiveness.

2. A neutron shield consisting of standard blocks will be more effective than one consisting of air dried blocks. The standard blocks are approximately 24.5 per cent more effective in slow neutron attenuation and approximately 6.4 per cent more effective in fast neutron attenuation than air dried blocks.

3. With haydite aggregate, standard concrete is more effective than standard mortar for neutron shielding. The concrete will be approximately 4.5 per cent more effective in shielding slow neutrons and 1.1 per cent more effective in shielding fast neutrons than a mortar.

4. In the air dried condition, with haydite aggregate, a mortar will be a more effective neutron shield than a concrete.

5. As the water content of a concrete is increased, the neutron attenuation will increase exponentially. The addition of 18 per cent water will decrease the slow neutron flux

by approximately 28.1 per cent and the fast neutron flux by approximately 8.61 per cent.

6. The fast neutron removal theory seems to yield valid results when used in predicting the change in shielding effectiveness of a concrete as the constituents of the concrete are changed.

7. The fast neutron removal theory will also predict the change in shielding effectiveness of a concrete for different amounts of absorbed water up to the maximum used in this study, 18 per cent by weight.

VIII. SUGGESTIONS FOR FURTHER STUDY

It was found in this study that the removal cross section theory was valid in predicting the fast neutron attenuation of concrete blocks containing absorbed water. A further study should be undertaken to determine if the theory remains valid in predicting the attenuation for even larger amounts of absorbed water. The lower limit of required water should also be determined for the continued validity of the theory.

Another useful study could be made of the gamma ray attenuation properties of haydite concrete in comparison with typical ordinary Portland cement concrete.

A study should also be made of the advantages of retaining water of crystallization, as in conventional concrete, compared with the retention of uncombined water absorbed in a spongy structure. The temperature at which the water of crystallization is lost might well be higher than that at which uncombined water evaporates.

IX. LITERATURE CITED

1. Albert, R. D. and Welton, T. A. Simplified theory of neutron attenuation and its application to reactor shield design. U.S. Atomic Energy Commission Report WAPD-15 (Del. [eted]) [Westinghouse. Atomic Power Division, Pittsburg, Pa.] . [Office of Technical Services, Washington, D.C.] November 30, 1950.

2. American Society for Testing Materials. 1955 book of A.S.T.M. standards. Part 3: Cement, concrete, ceramics. Philadelphia, Pa., Author. 1955.

3. Blizzard, E. P. and Miller, J. M. Radiation attenuation characteristics of structural concrete. U.S. Atomic Energy Commission Report ORNL-2193 [Oak Ridge National Lab., Tenn.] . [Office of Technical Services, Washington, D.C.] August 13, 1958.

4. Blosser, T. V. and associates. Study of the nuclear and physical properties of the ORNL graphite reactor shield. U.S. Atomic Energy Commission Report ORNL-1414 [Oak Ridge National Lab., Tenn.] . [Office of Technical Services, Washington, D.C.] August 21, 1958.

5. Gallaher, R. B. and Kitzes, A. S. Summary report on Portland cement concretes for shielding. U.S. Atomic Energy Commission Report ORNL-1414 [Oak Ridge National Lab., Tenn.] . [Office of Technical Services, Washington, D.C.] March 2, 1953.

6. Glasstone, S. Principles of nuclear reactor engineering. New York, N. Y., Van Nostrand Co., Inc. 1955.

7. ________ and Edlund, M. The elements of nuclear reactor theory. Princeton, N. J., Van Nostrand Co., Inc. 1956.

8. Goldstein, H. Attenuation of gamma rays and neutrons in reactor shield. Prepared by the Nuclear Development Corp. of America for the U.S. Atomic Energy Commission. Washington, D.C., U.S. Govt. Print. Off. 1957.

9. Hungerford, H. E. Shield materials. In the reactor handbook, Vol. 1, pp. 715-749. U.S. Atomic Energy Commission Report AECD-3647 [Technical Information

Service, AEC] . [Office of Technical Services, Washington, D.C.] 1955.

10. McMillan, F. R. Concrete primer. Detroit, Mich., American Concrete Institute. 1958.

11. Murray, R. Introduction to nuclear engineering. Englewood Cliffs, N. J., Prentice-Hall, Inc. 1954.

12. Price, B. T. and Horton, C. C. Radiation shielding. London, Pergamon Press, 1957.

13. Rockwell, T. Construction of cheap shields. U.S. Atomic Energy Commission Report AECD-3352 [Technical Information Service, AEC]. [Office of Technical Services, Washington, D.C.] January 16, 1950.

14. U.S. Housing and Home Finance Agency. Lightweight aggregate concretes. Washington, D.C., U.S. Govt. Print. Off. 1950.

X. ACKNOWLEDGMENTS

This study was part of the Nuclear Engineering-Nuclear Science curriculum offered by Iowa State College. Participation in this program was sponsored by the United States Navy Post Graduate School, Monterey, California.

My appreciation is extended to Dr. Glenn Murphy for his help, suggestions, criticism, and encouragement.

Thanks are extended to Dr. A. F. Voigt for the use of his equipment.

XI. APPENDIX: DATA FOR ADDITIONAL TESTS

Table 14. Compressive test data

Mixture	Standard Force lbs.	Standard Stress lbs./in.^{2}	Air dried Force lbs.	Air dried Stress lbs./in.^{2}
A	8440	2110	6520	1630
B	5640	1410	2270	568
C	4300	1075	1915	479
D	2705	676	1435	359
E	1740	435	1350	338
F	1497	374	850	213
G	3620	905	4335	1084
H	3220	805	3957	989
I	2530	633	3465	866

Table 15. Block orientation test

Face	Mixture A Counts	Mixture A Duration (min.)	Mixture A Count rate (CPM)	Mixture G Counts	Mixture G Duration (min.)	Mixture G Count rate (CPM)
1	21635	5	4327 ± 29	20060	5	4012 ± 28
2	21504	5	4301 ± 29	20325	5	4065 ± 28
3	21616	5	4323 ± 29	20242	5	4048 ± 28
4	21841	5	4368 ± 30	20417	5	4083 ± 29

Table 16. Detector shield replacement test

Run	Normal arrangement			Elevated arrangement		
	Counts	Duration (min.)	Count rate (CPM)	Counts	Duration (min.)	Count rate (CPM)
1	29816	5	5969 ± 34	36157	5	7231 ± 38
2	29761	5	5952 ± 34	36012	5	7202 ± 38
3	29745	5	5959 ± 34	36100	5	7220 ± 38
4	29749	5	5950 ± 34	36133	5	7227 ± 38

Table 17. Ice and paraffin tests

	Weight (gms.)	Slow neutron counts	Fast neutron counts
Ice	211.9	2604 ± 32	2078 ± 19
Paraffin	216.7	2558 ± 31	1998 ± 19